Table of contents

Experimental:

General:

Unless otherwise noted, all reagents were obtained commercially and without further purification before used. All moisture-sensitive compounds were manipulated using standard Schlenk line techniques. All moisture-sensitive reactions were conducted under a nitrogen atmosphere in glasswares that were oven-dried at 140 ^{o}C overnight prior to use. Anhydrous dimethylformamide (DMF) and diisopropylamine (DIPEA) were purchased from Acros. Other solvents were used as received. Merck silica gel 60 (70–230 mesh) was used for column chromatography. Handling of benzidine should be care since its potential linked to bladder and pancreatic cancer.

NMR spectra were recorded on a Bruker Ultrashield Advance Pro 400 MHz instrument and the chemical shifts were referenced internally to tetramethylsilane (TMS) or solvents in parts per million (ppm). UV-Visible absorption spectra were recorded with a HP UV-8453 spectrophotometer. Single-photon luminescence spectra were recorded using an Edinburgh Instrument FLSP920 spectrophotometer that was equipped with Xe900 continuous xenon lamp, µF920 microsecond flashlamp and a single photon counting Photomultiplier Tube. The excitation and emission spectra recorded on the FLSP920 were corrected with the correction file from the F900 software. CD spectra were recorded with a Jasco J-801 spectropolarimeter with a 0.1 mm cell at 25 ^{o}C and presented as Δε in $M^{-1}cm^{-1}$. HRMS were performed on a Agilent 6540 UHD Accurate-Mass Q-TOF LC/MS. Elemental analyses were performed on a Elementar Vario EL cube elemental analyzer. CPL were recorded on a Olis 17 UV/VIS/NIR/CD/CPL spectrophotometer On-Line Instrument Systems.

X-ray crystallography:

Measurements of crystal data were carried out on a Bruker Smart 1000 system equipped with an APEX II CCD device for **$[Eu_2(L1^{SS})_3](CF_3SO_3)_6$**, **$[Eu_2(L2^{RR})_3](CF_3SO_3)_6$** and **$L2^{RR}$** with graphite monochromated Mo-Kα radiation at room temperature. Multi-scan absorption correction was applied by SADABS program,[1] and the SAINT program was utilized for integration of the diffraction profiles.[2] The structures were solved by direct method and was refined by a full matrix least-squares treatment on F^2 using the SHELXTL programme system.[3] Structure **$[Eu_2(L2^{RR})_3](CF_3SO_3)_6$** contains highly disordered side arms, and were removed from the refinement using the PLATON/SQUEEZE program.[4] Although the side arms cannot be defined clearly, the helical structure was clearly observed. Crystal data, as well as details of data collection and refinement, are summarized in Table S2. Crystallographic data for the

structural analysis has been deposited with Cambridge Crystallographic Data Centre, CCDC No. for **$[Eu_2(L1^{SS})_3](CF_3SO_3)_6$** is 996693; No. for **$[Eu_2(L2^{RR})_3](CF_3SO_3)_6$** is 991735; No. for **$L2^{RR}$** is 1003776.

Synthesis:

(*R*)-6-(1-phenylethylcarbamoyl)picolinic acid 1^R and (*S*)-6-(1-phenylethyl carbamoyl)picolinic acid 1^S

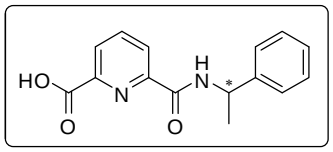

To a stirred solution of 2,6-pyridinedicarboxylic acid (5.00 g, 30.0 mmol, 2.5 equiv.) in anhydrous DMF (60 mL) at room temperature, HATU (4.56 g, 12.0 mmol, 1 equiv.) was added by five portions over 5 min under nitrogen. After allowing it to stir for 20 min, a (*R*)-1-phenylethylamine (1.83 mL, 14.4 mmol, 1.2 equiv.) was added dropwisely and the reaction mixture was allowed to stir for 20 min. DIPEA (5.50 mL, 31.6 mmol, 2.6 equiv.) was then added to the reaction mixture over 5 min and the resulting solution was stirred at room temperature for 14 h. The reaction mixture was then diluted with H_2O (100 mL), and extracted with DCM (5 × 30 mL), dried with $MgSO_4$, filtered, and concentrated *in vacuo*. The resulting residue was purified with flash column chromatography (with gradient from pure DCM to DCM/MeOH) to give a white solid. **1^R**: (2.40 g, 8.9 mmol, 74% yield), ^{1}H NMR (400 MHz, CD_3OD, 299 K, δ): 1.65 (dd, *J* = 16.0, 8 Hz, 3H), 5.26–5.32 (m, 1H), 7.25 (t, *J* = 8 Hz, 1H), 7.35 (t, *J* = 8 Hz, 2H), 7.46 (d, *J* = 4 Hz, 2H), 8.17 (t, *J* = 8 Hz, 1H), 8.33 (d, *J* = 8 Hz, 2H), 9.76 (d, *J* = 4 Hz, 1H). ^{13}C NMR (100.6 MHz, CD_3OD, 300 K, δ): 23.08, 51.46, 127.66, 128.14, 129.00, 129.37, 130.38, 141.35, 145.88, 148.88, 152.25, 165.66, 168.47. HRMS (ESI) calcd. for $C_{15}H_{14}N_2O_3Na$ $[M+Na]^+$: 293.0897, found 293.0895. The enantiomeric purity was determined with HPLC with AS-H column (Hexane/*i*-propanol: 80/20; flow rate: 1.0 ml/min) and compared with a racemic mixture according to the elution orders with retention times, t_S = 7.68 min and t_R = 14.27 min) to be 97% ee. **1^S** was isolated, following the procedure for **1^R** with the use of (*S*)-1-phenylethylamine instead, in 68% yield (2.20 g, 8.16 mmol): ^{1}H NMR (400 MHz, CD_3OD, 298 K, δ): 1.65 (d, *J* = 8 Hz, 3H), 5.30 (q, *J* = 8 Hz, 1H), 7.25 (t, *J* = 8 Hz, 1H), 7.35 (t, *J* = 8 Hz, 2H), 7.46 (d, *J* = 4 Hz, 2H), 8.16 (t, *J* = 8 Hz, 1H), 8.33 (dd, *J* = 8, 4 Hz, 2H), 9.76 (d, *J* = 8 Hz, 1H). ^{13}C NMR (100.6 MHz, CD_3OD, 300 K, δ): 23.07, 51.43, 127.64, 128.11, 128.98, 129.35, 130.35, 141.32, 145.85, 148.82, 152.20, 165.61, 168.43. HRMS (ESI) calcd. for $C_{15}H_{14}N_2O_3Na$ $[M+Na]^+$:

293.0897, found 293.0896. The enantiomeric purity was determined to be > 99% ee.

N,N'-(biphenyl-4,4'-diyl)bis[6-(*R*)-(1-phenylethylcarbamoyl)-pyridine-2-dicarboxamide] ($L1^{RR}$) and N,N'-(biphenyl-4,4'-diyl)bis[6-(*S*)-(1-phenylethylcarbamoyl)-pyridine-2-dicarboxamide] ($L1^{SS}$)

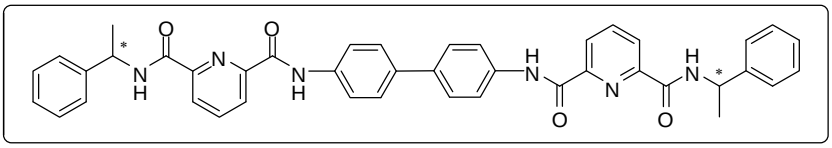

To a stirred solution of $\mathbf{1^R}$ (2.50 g, 9.26 mmol, 2.2 equiv.) in anhydrous DMF (40 mL) at room temperature, HATU (7.70 g, 20.3 mmol, 4.8 equiv.) was added under nitrogen. After allowing it to stir for 20 min, a benzidine (0.79 g, 4.27 mmol, 1.0 equiv.) was added and the reaction mixture was allowed to stir for 20 min in dark. DIPEA (9.24 mL, 53.03 mmol, 12.5 equiv.) was then added to the reaction mixture and the resulting solution was stirred at room temperature for 14 h. The reaction mixture was then diluted with H_2O (100 mL) and extracted with DCM (5 × 30 mL). After removing all of the organic volatile under reduced pressure, the residue was diluted with ethyl acetate (50 mL) and then washed with H_2O (5 × 30 mL) to remove the remained DMF. The organic layer was separated and then concentrated directly under reduced pressure. The residue was then diluted with MeCN (20 mL), and fine powder was progressively precipitated out. Then the solid was collected by filtration and the desired compound was isolated. **($L1^{RR}$)**: (2.53 g, 3.67 mmol, 86% yield), ^{1}H NMR (400 MHz, $(CD_3)_2SO$, 299 K, δ): 1.62 (d, *J* = 8 Hz, 6H), 5.25–5.31 (m, 2H), 7.23 (t, *J* = 8 Hz, 2H), 7.34 (t, *J* = 8 Hz, 4H), 7.45 (d, *J* = 8 Hz, 4H), 7.79 (d, *J* = 8 Hz, 4H), 7.93 (d, *J* = 8 Hz, 4H), 8.20–8.26 (m, 4H), 8.34 (d, *J* = 8 Hz, 2H), 9.60 (d, *J* = 8 Hz, 2H), 10.93 (s, 2H). ^{13}C NMR (100.6 MHz, $CD_3)_2SO$, 300 K, δ): 22.67, 49.08, 122.54, 125.79, 126.05, 127.02, 127.51, 127.69, 129.23, 136.38, 138.02, 140.62, 145.00, 149.58, 150.02, 162.62, 163.53. HRMS (ESI) calcd. for $C_{42}H_{36}N_6O_4Na$ $[M+Na]^+$: 711.2690, found 711.2681. **($L1^{SS}$)** was synthesized, following the procedure for **($L1^{RR}$)** with the use of $\mathbf{1^S}$ instead, in 80% yield (2.35 g, 3.42 mmol): ^{1}H NMR (400 MHz, $(CD_3)_2SO$, 299 K, δ): 1.61 (d, *J* = 8 Hz, 6H), 5.24–5.28 (m, 2H), 7.19 (t, *J* = 8 Hz, 2H), 7.30 (t, *J* = 8 Hz, 4H), 7.42 (d, *J* = 8 Hz, 4H), 7.75 (d, *J* = 8 Hz, 4H), 7.90 (d, *J* = 8 Hz, 4H), 8.18–8.21 (m, 4H), 8.31 (d, *J* = 8 Hz, 2H), 9.58 (d, *J* = 8 Hz, 2H), 10.91 (s, 2H). ^{13}C NMR (100.6 MHz, $CD_3)_2SO$, 300 K, δ): 22.74, 49.17, 122.62, 125.86, 126.12, 127.10, 127.58, 127.76, 129.30, 136.46, 138.10, 140.68, 145.08, 149.66, 150.10, 162.70, 163.62. HRMS (ESI) calcd. for $C_{42}H_{36}N_6O_4Na$ $[M+Na]^+$: 711.2690, found 711.2682.

{*N,N'*-(biphenyl-4,4'-diyl)bis[6-(*R*)-(1-phenylethyl-carbamoyl)-pyridine-2-dicarboxamide]}·2Eu·6(CF_3SO_3) [$Eu_2(L1^{RR})_3](CF_3SO_3)_6$ and 3{*N,N'*-(biphenyl-4,4'-diyl)bis[6-(*S*)-(1-phenylethylcarbamoyl)-pyridine-2-dicarboxamide]}·2Eu·6(CF_3SO_3) [$Eu_2(L1^{SS})_3](CF_3SO_3)_6$

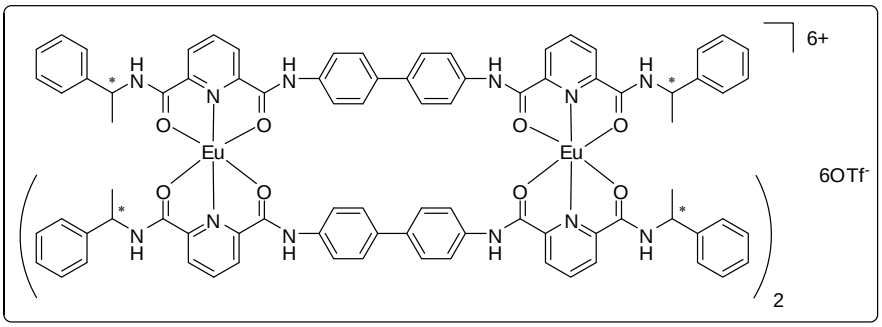

To a white suspension of **($L1^{RR}$)** (0.103 g, 0.150 mmol, 1.5 equiv.) in a mixture of 13 mL of DCM/MeOH (12:1, v/v), a solution of $Eu(CF_3SO_3)_3$ (0.060 g, 0.100 mmol, 1 equiv.) in 5 mL of MeCN was added. The suspension was changed to yellow turbidity immediately. The reaction mixture was then refluxed for 16 h and the solid progressively dissolved to give a resulting homogeneous yellow solution. The solvent was removed under reduced pressure. The solid was then washed with THF to give the desired product. **[$Eu_2(L1^{RR})_3](CF_3SO_3)_6$**: (0.140 g, 0.043 mmol, 85% yield) ^{1}H NMR (400 MHz, CD_3CN, 298 K, δ): 1.54 (s, br., 3 × 6H, C*H*$_3$), 4.95 (s, br., 3 × 2H, N-*H*), 5.27 (s, br., 3 × 2H, (CH_3)C*H*), 6.36 (s, br., 3 × 4H), 6.71 (s, br., 3 × 4H, phenyl-*H*), 6.77 (s, br., 3 × 4H, phenyl-*H*), 6.83 (s, br., 3 × 6H), 6.95 (s, br., 3 × 2H, N-*H*), 7.09 (s, br. 3 × 2H), 7.87 (s, br. 3 × 4H, phenyl-*H*). ^{13}C NMR (100.6 MHz, CD_3CN, 298 K, δ): 22.45 (*C*H$_3$), 52.30 (*C*H), 93.11, 93.62, 123.32, 126.44, 128.14, 128.35, 129.44, 136.95, 139.06, 143.68, 144.82, 145.70, 156.35, 161.81 (*C*O), 165.23 (*C*O). HRMS (ESI) calcd. for $C_{130}H_{108}N_{18}Eu_2O_{24}S_4F_{12}$ $[M\text{-}2OTf]^{2+}$: 1481.2431 (^{151}Eu based), found 1481.2432. Calculated for $C_{132}H_{108}N_{18}O_{30}Eu_2F_{18}S_6{\cdot}2H_2O$: C, 48.03; H, 3.42; N, 7.64%; Found: C, 47.24; H, 3.37; N, 7.47 %; **[$Eu_2(L1^{SS})_3](CF_3SO_3)_6$** was synthesized, following the procedure for **[$Eu_2(L1^{RR})_3](CF_3SO_3)_6$** with the use of **($L1^{SS}$)** instead, in 92% yield (0.150 g, 0.046 mmol): ^{1}H NMR (400 MHz, CD_3CN, 299 K, δ): 1.53 (s, br., 3 × 6H, C*H*$_3$), 4.92 (s, br., 3 × 2H, N-*H*), 5.25 (s, br., 3 × 2H, (CH_3)C*H*), 6.36 (s, br., 3 × 4H), 6.70 (s, br., 3 × 4H, phenyl-*H*), 6.74 (s, br., 3 × 4H, phenyl-*H*), 6.82 (s, br., 3 × 6H), 6.92 (s, br., 3 × 2H, N-*H*), 7.07 (s, br. 3 × 2H), 7.85 (s, br. 3 × 4H, phenyl-*H*). ^{13}C NMR (100.6 MHz, CD_3CN, 300 K, δ): 22.46 (*C*H$_3$), 52.37 (*C*H), 93.34, 93.80, 123.35, 126.52, 128.19, 128.44, 129.51, 136.93, 139.12, 143.63, 144.90, 145.77, 156.35, 161.83 (*C*O), 165.23 (*C*O). HRMS (ESI) calcd. for $C_{130}H_{108}N_{18}Eu_2O_{24}S_4F_{12}$ $[M\text{-}2OTf]^{2+}$: 1481.2431 (^{151}Eu based), found 1481.2433. Calculated for $C_{132}H_{108}N_{18}O_{30}Eu_2F_{18}S_6{\cdot}2H_2O$: C, 48.03; H, 3.42; N,

7.64%; Found: C, 47.49; H, 3.42; N, 7.54 %.

3{*N,N'*-(biphenyl-4,4'-diyl)bis[6-(*R*)-(1-phenylethyl-carbamoyl)-pyridine-2-dicarboxamide]}·2La·6(CF_3SO_3) [$La_2(L1^{RR})_3](CF_3SO_3)_6$ and 3{*N,N'*-(biphenyl-4,4'-diyl)bis[6-(*S*)-(1-phenylethylcarbamoyl)-pyridine-2-dicarboxamide]}·2La·6(CF_3SO_3) [$La_2(L1^{SS})_3](CF_3SO_3)_6$

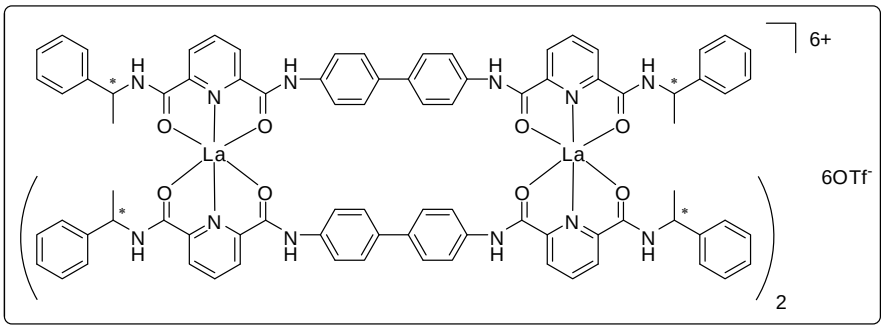

To a white suspension of **($L1^{RR}$)** (0.050 g, 0.073 mmol, 1.5 equiv.) in a mixture of 6 mL of DCM/MeOH (12:1, v/v), a solution of $La(CF_3SO_3)_3$ (0.028 g, 0.048 mmol, 1 equiv.) in 3 mL of MeCN was added. The suspension was changed to yellow turbidity immediately. The reaction mixture was then refluxed for 16 h and the solid progressively dissolved to give a resulting homogeneous yellow solution. The solvent was removed under reduced pressure. The solid was then washed with THF to give the desired product. **[$La_2(L1^{RR})_3](CF_3SO_3)_6$**: (0.071 g, 0.022 mmol, 93% yield) ^{1}H NMR (400 MHz, CD_3CN, 298 K, δ): 1.75 (d, *J* = 8 Hz, 3 × 6H, C*H*$_3$), 5.08–5.16 (m, 3 × 2H, (CH_3)C*H*), 6.64 (d, *J* = 8 Hz, 3 × 4H, phenyl-*H*), 7.11–7.17 (m, 3 × 4H, phenyl-*H*), 7.18–7.23 (overlapping of two type of peaks, m, 3 × 4H, phenyl-*H* and m, 3 × 2H), 7.71 (d, *J* = 8 Hz, 3 × 4H, phenyl-*H*), 8.50–8.55 (m, 3 × 4H), 8.56–8.60 (m, 3 × 2H), 9.09 (d, *J* = 8 Hz, 3 × 2H, N-*H*), 10.32 (s, 3 × 2H, N-*H*). ^{13}C NMR (100.6 MHz, CD_3CN, 298 K, δ): 22.15 (*C*H$_3$), 53.71 (*C*(CH_3)H), 122.86 (*C*H), 127.38 (*C*H), 127.93 (*C*H), 128.63 (*C*H), 129.08 (*C*H), 130.05 (*C*H), 136.86, 139.19, 143.17, 144.54 (*C*H), 150.14, 150.79, 168.12 (*C*O), 168.95 (*C*O). HRMS (ESI) calcd. for $C_{129}H_{108}N_{18}La_2O_{21}S_3F_9$ [M-3OTf]$^{3+}$: 929.8355, found 929.8354. Calculated for $C_{132}H_{108}N_{18}O_{30}La_2F_{18}S_6{\cdot}5H_2O{\cdot}2CH_3OH$: C, 47.44; H, 3.74; N, 7.43%; Found: C, 46.14; H, 3.72; N, 7.32 %; **[$La_2(L1^{SS})_3](CF_3SO_3)_6$** was synthesized, following the procedure for **[$La_2(L1^{RR})_3](CF_3SO_3)_6$** with the use of **($L1^{SS}$)** instead: (0.070 g, 0.022 mmol, 90% yield) ^{1}H NMR (400 MHz, CD_3CN, 298 K, δ): 1.75 (d, *J* = 8 Hz, 3 × 6H, C*H*$_3$), 5.09–5.16 (m, 3 × 2H, (CH_3)C*H*), 6.64 (d, *J* = 8 Hz, 3 × 4H, phenyl-*H*), 7.12–7.16 (m, 3 × 4H, phenyl-*H*), 7.18–7.23 (m, 3 × 4H, phenyl-*H;* m, 3 × 2H), 7.71 (d, *J* = 8 Hz, 3 × 4H, phenyl-*H*), 8.51 (t, *J* = 8 Hz, 3 × 2H), 8.56 (d, *J* = 8 Hz, 3 × 2H), 8.60 (d, *J* = 8 Hz, 3 × 2H), 9.09 (d, *J* = 8 Hz, 3 × 2H, N-*H*), 10.32 (s, 3 × 2H, N-*H*). ^{13}C

NMR (100.6 MHz, CD_3CN, 299 K, δ): 22.16 (*C*H_3), 53.73 (*C*(CH_3)H), 122.88 (*C*H), 127.41 (*C*H), 127.96 (*C*H), 128.65 (*C*H), 129.11 (*C*H), 130.08 (*C*H), 136.87, 139.22, 143.18, 144.57 (*C*H), 150.16, 150.81, 168.15 (*C*O), 168.98 (*C*O). HRMS (ESI) calcd. for $C_{129}H_{108}N_{18}La_2O_{21}S_3F_9$ $[M\text{-}3OTf]^{3+}$: 929.8355, found 929.8352.. Calculated for $C_{132}H_{108}N_{18}O_{30}La_2F_{18}S_6{\cdot}4H_2O$: C, 47.89; H, 3.53; N, 7.62%; Found: C, 47.45; H, 3.46; N, 7.53 %.

(*R*)-6-(2-phenylpropylcarbamoyl)picolinic acid 2^R or (*S*)-6-(2-phenylpropyl carbamoyl)picolinic acid 2^S

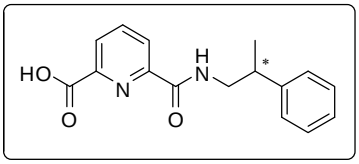

To a stirred solution of 2,6-pyridinedicarboxylic acid (9.89 g, 59.1 mmol, 4.0 equiv.) in anhydrous DMF (130 mL) at room temperature, HATU (5.64 g, 14.8 mmol, 1.0 equiv.) was added by portions over 10 min under nitrogen. After allowing it to stir for 20 min, a (*R*)-β-methylphenethylamine (2.11 mL, 14.83 mmol, 1.0 equiv.) was added dropwisely and the reaction mixture was allowed to stir for 20 min. DIPEA (5.68 mL, 32.6 mmol, 2.2 equiv.) was then added to the reaction mixture over 5 min and the resulting solution was stirred at room temperature for 18 h. The reaction mixture was then diluted with H_2O (200 mL), and extracted with DCM (5 × 50 mL), dried with $MgSO_4$, filtered, and concentrated *in vacuo*. The resulting residue was purified with flash column chromatography (DCM/EtOH 12:1, v/v) to give a white solid. **2^R**: (1.93 g, 6.8 mmol, 46% yield) ^{1}H NMR (400 MHz, CD_3OD, 299 K, δ): 1.35 (d, *J* = 8.0 Hz, 3H), 3.17 (qin, *J* = 8 Hz, 1H), 3.61 (d, *J* = 8 Hz, 2H), 7.18–7.22 (m, 1H), 7.28–7.32 (m, 4H), 8.15 (t, *J* = 8 Hz, 1H), 8.30 (d, *J* = 8 Hz, 2H), 9.42 (m, 1H). ^{13}C NMR (100.6 MHz, CD_3OD, 300 K, δ): 20.46, 41.80, 48.58, 127.34, 128.37, 129.05, 129.15, 130.36, 141.30, 146.59, 148.81, 151.99, 166.50, 168.28. HRMS (ESI) calcd. for $C_{16}H_{16}N_2O_3Na$ $[M+Na]^+$: 307.1053, found 307.1053. The enantiomeric purity was determined with HPLC with AS-H column (Hexane/*i*-propanol: 80/20; flow rate: 0.25 ml/min) and compared with a racemic mixture according to the elution orders with retention times, t_S = 46.33 min and t_R = 49.46 min) to be 88% ee. **2^S** was isolated, following the procedure for **2^R** with the use of (*S*)-β-methylphenethylamine instead, in 43% yield (1.81 g, 6.36 mmol): ^{1}H NMR (400 MHz, CD_3OD, 299 K, δ): 1.36 (d, *J* = 8.0 Hz, 3H), 3.17 (qin, *J* = 8 Hz, 1H), 3.62 (d, *J* = 8 Hz, 2H), 7.19–7.22 (m, 1H), 7.28–7.31 (m, 4H), 8.15 (t, *J* = 8 Hz, 1H), 8.31 (d, *J* = 4 Hz, 2H). ^{13}C NMR (100.6 MHz, CD_3OD, 300

K, δ): 20.46, 41.81, 48.60, 127.34, 128.38, 129.06, 129.16, 130.37, 141.32, 146.60, 148.83, 152.00, 166.51, 168.29. HRMS (ESI) calcd. for $C_{16}H_{16}N_2O_3Na$ $[M+Na]^+$: 307.1053, found 307.1052. The enantiomeric purity was determined to be 96% ee.

N,N'-(biphenyl-4,4'-diyl)bis[6-(*R*)-(2-phenylpropylcarbamoyl)-pyridine-2,6-dicarboxamide] (L2^{RR}) and N,N'-(biphenyl-4,4'-diyl)bis[6-(*S*)-(2-phenylpropylcarbamoyl)-pyridine-2,6-dicarboxamide] (L2^{SS})

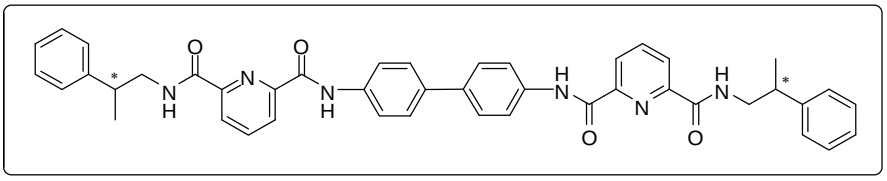

To a stirred solution of **2^R** (1.00 g, 3.52 mmol, 2.2 equiv.) in anhydrous DMF (16 mL) at room temperature, HATU (2.93 g, 7.69 mmol, 4.8 equiv.) was added under nitrogen. After allowing it to stir for 20 min, a benzidine (0.30 g, 1.61 mmol, 1.0 equiv.) was added and the reaction mixture was allowed to stir for 20 min in dark. DIPEA (3.51 mL, 20.16 mmol, 12.5 equiv.) was then added to the reaction mixture and the resulting solution was stirred at room temperature for 14 h. The reaction mixture was then diluted with H_2O (20 mL) and extracted with DCM (5 × 30 mL). After removing all of the organic volatile under reduced pressure, the residue was diluted with ethyl acetate (20 mL) and then washed with H_2O (5 × 30 mL) to remove the remained DMF. The organic layer was separated and concentrated directly under reduced pressure. The residue was then diluted with MeCN (20 mL), and fine powder was progressively precipitated out. Then the solid was collected by filtration and the desired compound was isolated. **(L2^{RR})**: (0.42 g, 0.588 mmol, 73% yield), ^{1}H NMR (400 MHz, $CDCl_3$, 299K, δ): 1.42 (d, *J* = 8 Hz, 6H), 3.11–3.17 (m, 2H), 3.48–3.54 (m, 2H), 4.00–4.06 (m, 2H), 7.26–7.31 (m, 2H), 7.34–7.42 (m, 8H), 7.60–7.69 (m, 10H), 8.09 (t, *J* = 8 Hz, 2H), 8.41 (d, *J* = 8 Hz, 2H), 8.44 (d, *J* = 8 Hz, 2H), 9.20 (s, 2H). ^{13}C NMR (100.6 MHz, $CDCl_3$, 300 K, δ): 19.31, 39.97, 45.96, 120.70, 125.21, 125.45, 127.14, 127.31, 127.35, 128.95, 136.29, 136.89, 139.33, 143.91, 148.63, 148.88, 161.10, 163.09. HRMS (ESI) calcd. for $C_{44}H_{40}N_6O_4Na$ $[M+Na]^+$: 739.3003, found 739.2994. **(L2^{SS})** was isolated, following the procedure for **(L2^{RR})** with the use of **2^S** instead, in 69% yield (0.40 g, 0.555 mmol): ^{1}H NMR (400 MHz, $CDCl_3$, 298K, δ): 1.42 (d, *J* = 8 Hz, 6H), 3.13–3.15 (m, 2H), 3.48–3.53 (m, 2H), 4.01–4.06 (m, 2H), 7.27–7.31 (m, 2H), 7.35–7.42 (m, 8H), 7.58–7.60 (m, 2H), 7.65–7.70 (m, 8H), 8.10 (t, *J* = 8 Hz, 2H), 8.41 (d, *J* = 8 Hz, 2H), 8.45 (d, *J* = 8 Hz, 2H), 9.19 (s, 2H). ^{13}C NMR (100.6 MHz, $CDCl_3$, 298K, δ): 19.32, 39.99, 45.96, 120.71, 125.24, 125.48, 127.17, 127.35, 127.37, 128.97,

136.30, 136.94, 139.36, 143.92, 148.63, 148.88, 161.11, 163.02. HRMS (ESI) calcd. for $C_{44}H_{40}N_6O_4Na$ $[M+Na]^+$: 739.3003, found 739.2996.

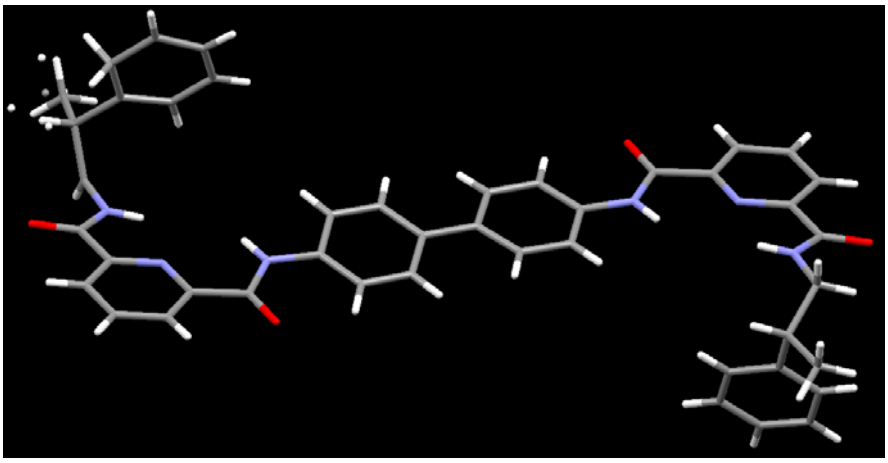

Figure S1. X-ray crystallography of **L2^{RR}** showing transoid conformation of the pyridine-*N* and its neighbor carbonyl-*O*s.

3{ *N*,*N*′-(biphenyl-4,4′-diyl)bis[6-(*R*)-(2-phenylpropylcarbamoyl)-pyridine-2,6-dicarboxamide]}·2Eu·6(CF_3SO_3) [Eu_2(L2^{RR})$_3$](CF_3SO_3)$_6$ and 3{ *N*,*N*′-(biphenyl-4,4′-diyl)bis[6-(*S*)-(2-phenylpropylcarbamoyl)-pyridine-2,6-dicarboxamide]}·2Eu·6(CF_3SO_3) [Eu_2(L2^{SS})$_3$](CF_3SO_3)$_6$

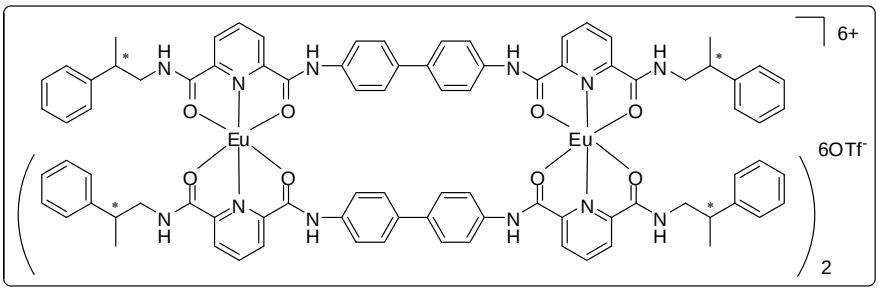

To a white suspension of **(L2^{RR})** (0.107 g, 0.150 mmol, 1.5 equiv.) in a mixture of 13 mL of DCM/MeOH (12:1, v/v), a solution of $Eu(CF_3SO_3)_3$ (0.060 g, 0.100 mmol, 1 equiv.) in 5 mL of MeCN was added. The solution was changed to yellow turbidity immediately. The solution was then refluxed and the solid progressively dissolved to give a resulting homogeneous yellow solution. After for 16 h, the solvent was removed under reduced pressure. The solid was then washed with DCM to give the desired product. **[Eu_2(L2^{RR})$_3$](CF_3SO_3)$_6$**: (0.154 g, 0.046 mmol, 91% yield), ^{1}H NMR (400 MHz, CD_3CN, 298 K, some of the peaks are shown two sets of peaks, **A** and **B**,

respectively in ~ 1.1:1 ratio, δ): 1.02 (s, br., 3 × 6H, **C*H₃*, A**), 1.33 (s, br., 3 × 6H, **C*H₃*, B**), 2.56 (s, br., 3 × 2H, (CH_3)**C*H*, A**), 2.96 (s, br., 3 × 2H, (CH_3)**C*H*, B**), 3.77 (overlapping of three type of peaks, br. 3 × 2H, **C*H*H**, **A**, 3 × 2H, **CH*H***, **A** and 3 × 2H, **CH*H***, **B**), 4.01 (s, br. 3 × 2H, **C*H*H**, **B**), 4.82 (s, br. 3 × 2H, **N*H***, **A**), 4.96 (s, br. 3 × 2H, **N*H***, **B**), 6.36 (s, br. 3 × 4H, **A**), 6.64 (m, br. 3 × 4H, **B**), 7.06–7.31 (m, br. 3 × 18H, **A** and 3 × 18H **B**), 8.36 (s, br. 3 × 4H, **A**), 8.44 (s, br. 3 × 4H, **B**). ^{13}C NMR (100.6 MHz, CD_3CN, 298 K, some of the peaks are shown two sets of peaks, δ): 19.35 (***C*H₃**), 19.63 (***C*H₃**), 41.00 (***C*H**), 41.29 (***C*H**), 47.94 (***C*H₂**), 47.96 (***C*H₂**), 93.07, 93.09, 93.59, 93.89, 123.63, 127.71, 127.90, 128.00, 128.41, 128.48, 129.62, 129.70, 137.26, 137.30, 139.33, 139.38, 144.36, 144.41, 144.55, 145.42, 145.88, 156.35, 161.94 (***C*O**), 162.38 (***C*O**), 165.13 (***C*O**), 165.26 (***C*O**). HRMS (ESI) calcd. for $C_{136}H_{120}N_{18}Eu_2O_{24}S_4F_{12}$ $[M\text{-}2OTf]^{2+}$: 1523.2900 (^{151}Eu based), found 1523.2905. Calculated for $C_{138}H_{120}N_{18}O_{30}Eu_2F_{18}S_6{\cdot}2H_2O$: C, 48.97; H, 3.69; N, 7.45%; Found: C, 48.47; H, 3.63; N, 7.36 %; **$[Eu_2(L2^{SS})_3](CF_3SO_3)_6$** was synthesized, following the procedure for **$[Eu_2(L2^{RR})_3](CF_3SO_3)_6$** with the use of **($L2^{SS}$)** instead, in 92% yield (0.154 g, 0.046 mmol): ^{1}H NMR (400 MHz, CD_3CN, 297 K, some of the signals are shown in two sets of peaks, **A** and **B**, respectively in ~ 1.1:1 ratio, δ): 0.90 (s, br., 3 × 6H, **C*H₃*, A**), 1.32 (s, br., 3 × 6H, **C*H₃*, B**), 2.54 (s, br., 3 × 2H, **C*H*, A**), 2.96 (s, br., 3 × 2H, **C*H*, B**), 3.74 (s, br. 3 × 2H, **C*H*H**, **A**), 3.78 (s, br., 3 × 2H, **CH*H***, **A** and 3 × 2H, **CH*H***, **B**), 4.02 (s, br. 3 × 2H, **C*H*H**, **B**), 4.73 (s, br. 3 × 2H, **N*H***, **A**), 4.87 (s, br. 3 × 2H, **N*H***, **B**), 6.33 (s, br. 3 × 4H, **A**), 6.64 (m, br. 3 × 4H, **B**), 7.07–7.31 (m, br. 3 × 18H, **A** and m, br. 3 × 18H **B**), 8.37 (s, br. 3 × 4H, **A**), 8.45 (s, br. 3 × 4H, **B**). ^{13}C NMR (100.6 MHz, CD_3CN, 298 K, some of the peaks are shown into two sets of peaks, δ): 19.35 (***C*H₃**), 19.63 (***C*H₃**), 41.00 (***C*H**), 41.29 (***C*H**), 47.93 (***C*H₂**), 47.98 (***C*H₂**), 93.13, 93.18, 93.71, 93.91, 123.63, 127.88, 127.91, 128.00, 128.41, 128.49, 129.62, 129.70, 137.23, 137.27, 139.34, 139.39, 144.36, 144.40, 144.60, 145.43, 145.90, 156.32, 161.91 (***C*O**), 162.36 (***C*O**), 165.13 (***C*O**), 165.26 (***C*O**). HRMS (ESI) calcd. for $C_{136}H_{120}N_{18}Eu_2O_{24}S_4F_{12}$ $[M\text{-}2OTf]^{2+}$: 1523.2900 (^{151}Eu based), found 1523.2889. Calculated for $C_{138}H_{120}N_{18}O_{30}Eu_2F_{18}S_6{\cdot}2H_2O$: C, 48.97; H, 3.69; N, 7.45%; Found: C, 48.24; H, 3.60; N, 7.31 %.

3{ *N,N'*-(biphenyl-4,4'-diyl)bis[6-(*R*)-(2-phenylpropylcarbamoyl)-pyridine-2,6-dicarboxamide]}·2La·6(CF_3SO_3) $[La_2(L2^{RR})_3](CF_3SO_3)_6$ and 3{ *N,N'*-(biphenyl-4,4'-diyl)bis[6-(*S*)-(2-phenylpropylcarbamoyl)-pyridine-2,6-dicarboxamide]}·2La·6(CF_3SO_3) $[La_2(L2^{SS})_3](CF_3SO_3)_6$

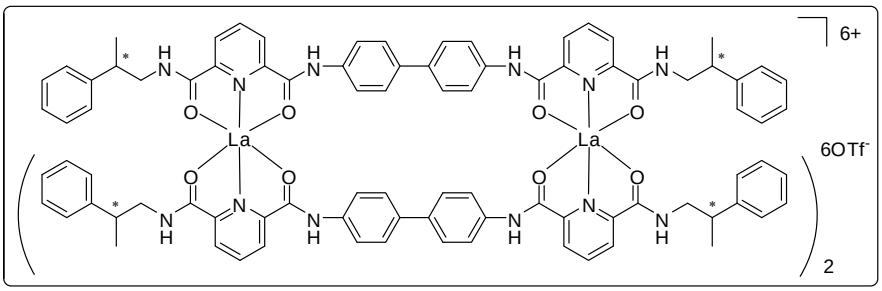

To a white suspension of **(L2^{RR})** (0.040 g, 0.056 mmol, 1.5 equiv.) in a mixture of 6 mL of DCM/MeOH (8:1, v/v), a solution of $La(CF_3SO_3)_3$ (0.022 g, 0.037 mmol, 1 equiv.) in 8 mL of MeCN was added. The suspension was changed to yellow turbidity immediately. The reaction mixture was then refluxed for 16 h and the solid progressively dissolved to give a resulting homogeneous yellow solution. The solvent was removed under reduced pressure. The solid was then washed with DCM to give the desired product. **$[La_2(L2^{RR})_3](CF_3SO_3)_6$**: (0.055 g, 0.016 mmol, 89% yield) ^{1}H NMR (400 MHz, CD_3CN, 298 K, some of the signals are shown in two sets of peaks, **A** and **B**, respectively in ~1:1.1 ratio, δ): 1.02 (s, br., 3 × 6H, A), 1.18 (s, br., 3 × 6H, B), 2.77 (s, br., 3 × 2H, B), 2.93 (s, br., 3 × 2H, A), 3.40 (s, br., 3 × 6H), 3.57 (s, br., 3 × 2H), 6.72 (s, br. 3 × 8H, A), 7.05 (s, br., 3 × 8H, B), 7.18–7.30 (m, 3 × 12H), 7.82 (s, br. 3 × 8H), 8.40 (s, br., 3 × 4H, B), 8.59 (s, br., 3 × 4H, A), 8.75 (s, br., 3 × 4H, B), 8.87 (s, br., 3 × 4H, A), 10.47 (s, br., 3 × 4H). ^{13}C NMR (100.6 MHz, CD_3CN, 298 K, some of the peaks cannot be shown clearly due to limited solubility, δ): 19.85, 19.90, 40.29, 40.51, 49.19, 49.31, 122.97, 123.00, 127.29, 127.35, 128.26, 128.33, 128.46, 128.78, 130.11, 137.01, 139.29, 144.82, 144.89, 150.43, 151.16, 151.30. HRMS (ESI) calcd. for $C_{135}H_{120}N_{18}La_2O_{21}S_3F_9$ $[M\text{-}3OTf]^{3+}$: 957.8668, found 957.8670. Calculated for $C_{138}H_{120}N_{18}O_{30}La_2F_{18}S_6{\cdot}4H_2O$: C, 48.83; H, 3.80; N, 7.43%; Found: C, 48.02; H, 3.73; N, 7.30 %; **$[La_2(L2^{SS})_3](CF_3SO_3)_6$** was synthesized, following the procedure for **$[La_2(L2^{RR})_3](CF_3SO_3)_6$** with the use of **(L2^{SS})** instead, in 85% yield (0.052 g, 0.016 mmol): ^{1}H NMR (400 MHz, CD_3CN, 298 K, some of the signals are shown in two sets of peaks, **A** and **B**, respectively in ~1:1.1 ratio, δ): 1.02 (s, br., 3 × 6H, A), 1.16 (s, br., 3 × 6H, B), 2.77 (s, br., 3 × 2H, B), 2.93 (s, br., 3 × 2H, A), 3.39 (s, br., 3 × 6H), 3.57 (s, br., 3 × 2H), 6.72 (s, br. 3 × 8H, A), 7.04 (s, br., 3 × 8H, B), 7.17–7.39 (m, 3 × 12H), 7.82 (s, br. 3 × 8H), 8.40 (s, br., 3 × 4H, B), 8.58 (s, br., 3 × 4H, A), 8.75 (s, br., 3 × 4H, B), 8.89 (s, br., 3 × 4H, A), 10.47 (s, br., 3 × 4H). ^{13}C NMR (100.6 MHz, CD_3CN, 298 K, some of the peaks cannot be shown clearly due to limited solubility, δ): 19.87, 40.24, 40.49, 49.14, 49.37, 122.91, 123.05, 127.32, 128.28, 128.49, 128.76, 130.14, 134.20, 137.02, 139.36, 144.86, 150.44, 151.33, 168.23, 168.41. HRMS (ESI) calcd. for $C_{135}H_{120}N_{18}La_2O_{21}S_3F_9$ $[M\text{-}3OTf]^{3+}$: 957.8668, found 957.8662. Calculated for $C_{138}H_{120}N_{18}O_{30}La_2F_{18}S_6{\cdot}4H_2O$: C, 48.83; H, 3.80; N, 7.43%; Found: C, 48.00; H, 3.78; N,

7.31 %.

3{ *N,N'*-(biphenyl-4,4'-diyl)bis[6- (*S*)-(2-phenylpropylcarbamoyl)-pyridine-2,6-dicarboxamide]}·2Gd·6(CF_3SO_3) [$Gd_2(L2^{SS})_3](CF_3SO_3)_6$

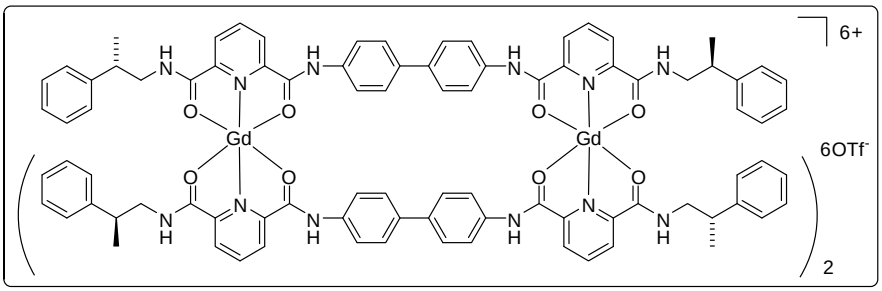

To a white suspension of **($L2^{SS}$)** (0.050 g, 0.056 mmol, 1.5 equiv.) in a mixture of 6 mL of DCM/MeOH (12:1, v/v), a solution of $Gd(CF_3SO_3)_3$ (0.028 g, 0.047 mmol, 1 equiv.) in 8 mL of MeCN was added. The suspension was changed to yellow turbidity immediately. The reaction mixture was then refluxed for 16 h and the solid progressively dissolved to give a resulting homogeneous yellow solution. The solvent was removed under reduced pressure. The solid was then washed with DCM to give the desired product. **[$Gd_2(L2^{SS})_3](CF_3SO_3)_6$**: (0.071 g, 0.021 mmol, 90% yield) HRMS (ESI) calcd. for $C_{135}H_{120}N_{18}Gd_2O_{21}S_3F_9$ $[M\text{-}3OTf]^{3+}$: 970.5464, found 970.5457.

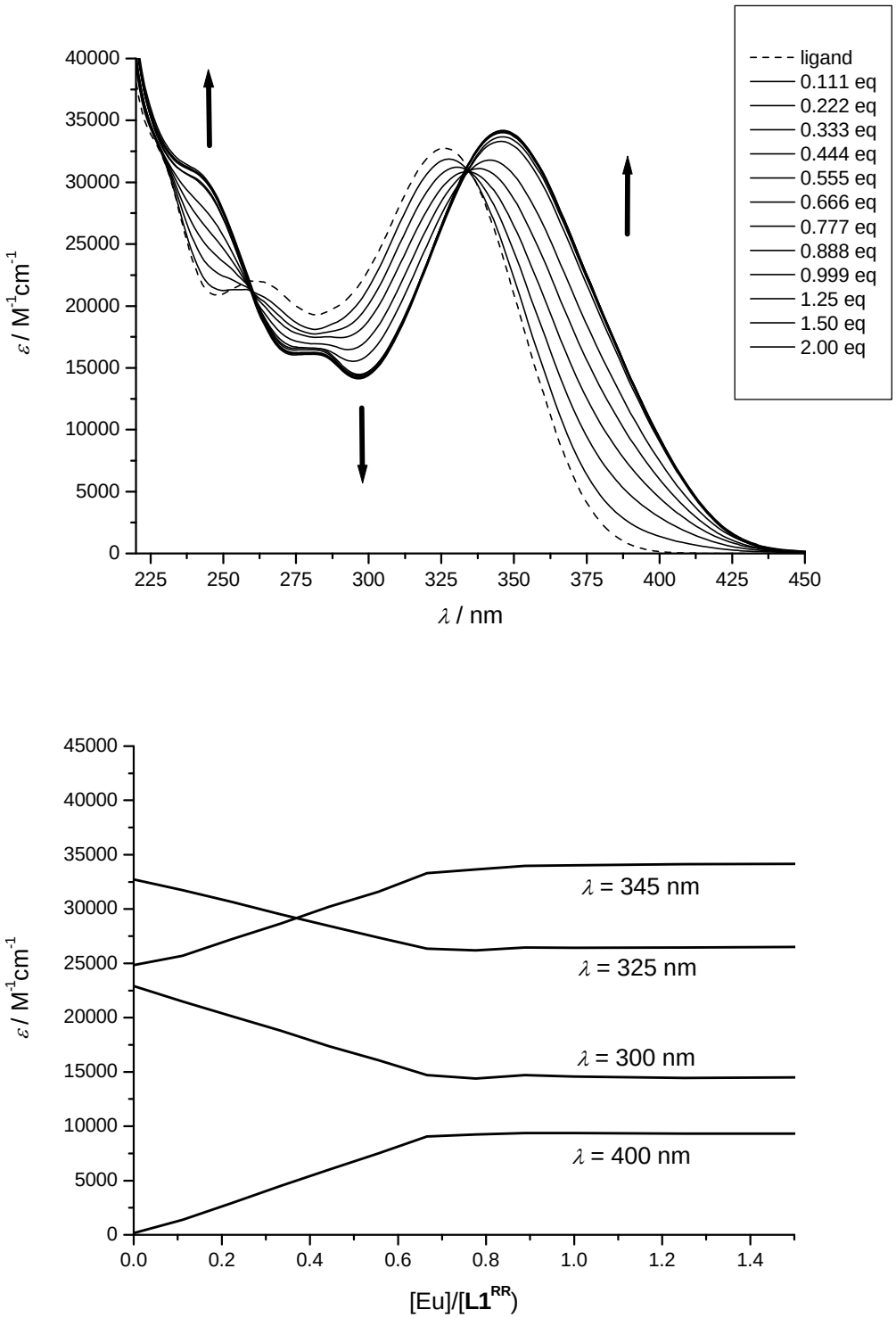

Figure S2. (Upper) Variation in UV-Vis absorption spectra of titrating **L1^{RR}** (1.72×10^{-4} M, in 73:3:24, v/v/v, of $CHCl_3$/MeOH/MeCN) with $Eu(OTf)_3$ (0.038M in MeCN) at 298 K (Eu:**L1^{RR}** = 0.0–2.0). (Lower) Variation of molar extinction coefficients at four different wavelengths upon titrating **L1^{RR}** with $Eu(OTf)_3$.

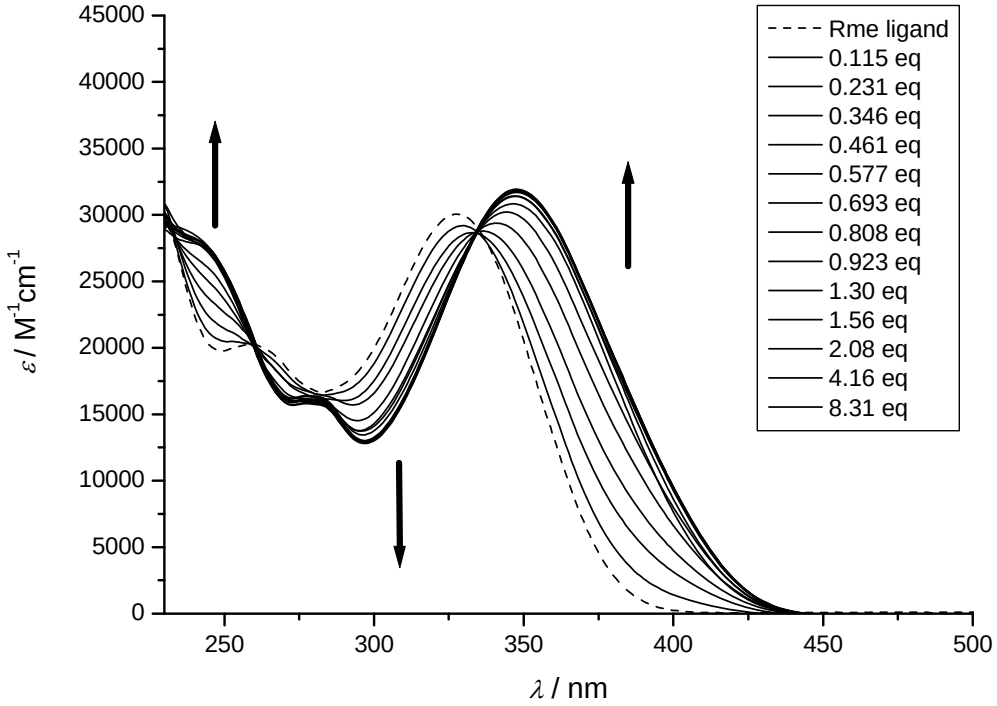

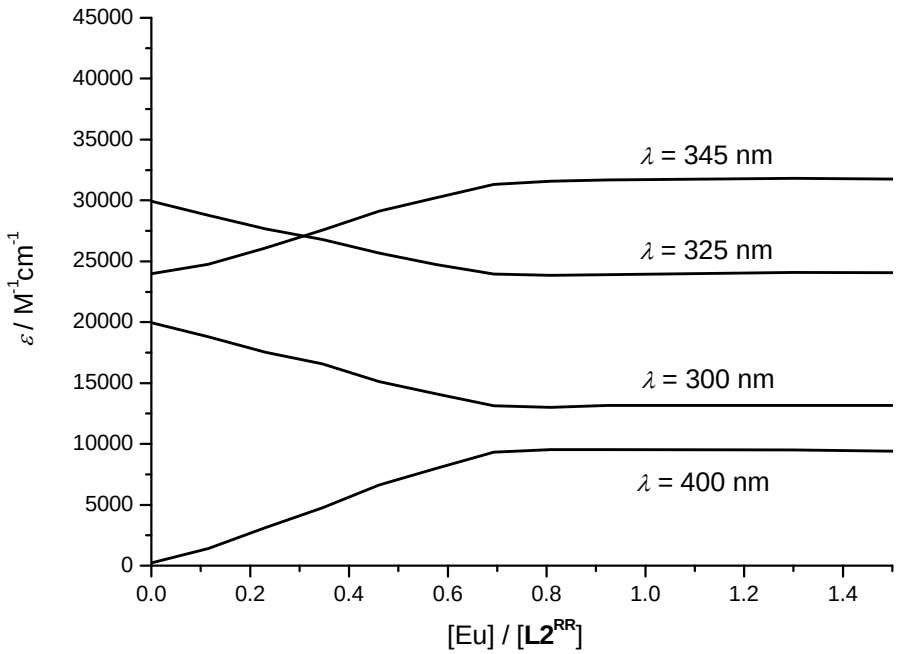

Figure S3. (Upper) Variation in UV-Vis absorption spectra of titrating **L2^{RR}** (1.65×10^{-4} M, in 73:3:24, v/v/v, of $CHCl_3$/MeOH/MeCN) with $Eu(OTf)_3$ (0.038M in MeCN) at 298 K (Eu:**L2^{RR}** = 0.0–2.0). (Lower) Variation of molar extinction coefficients at four different wavelengths upon titrating **L2^{RR}** with $Eu(OTf)_3$.

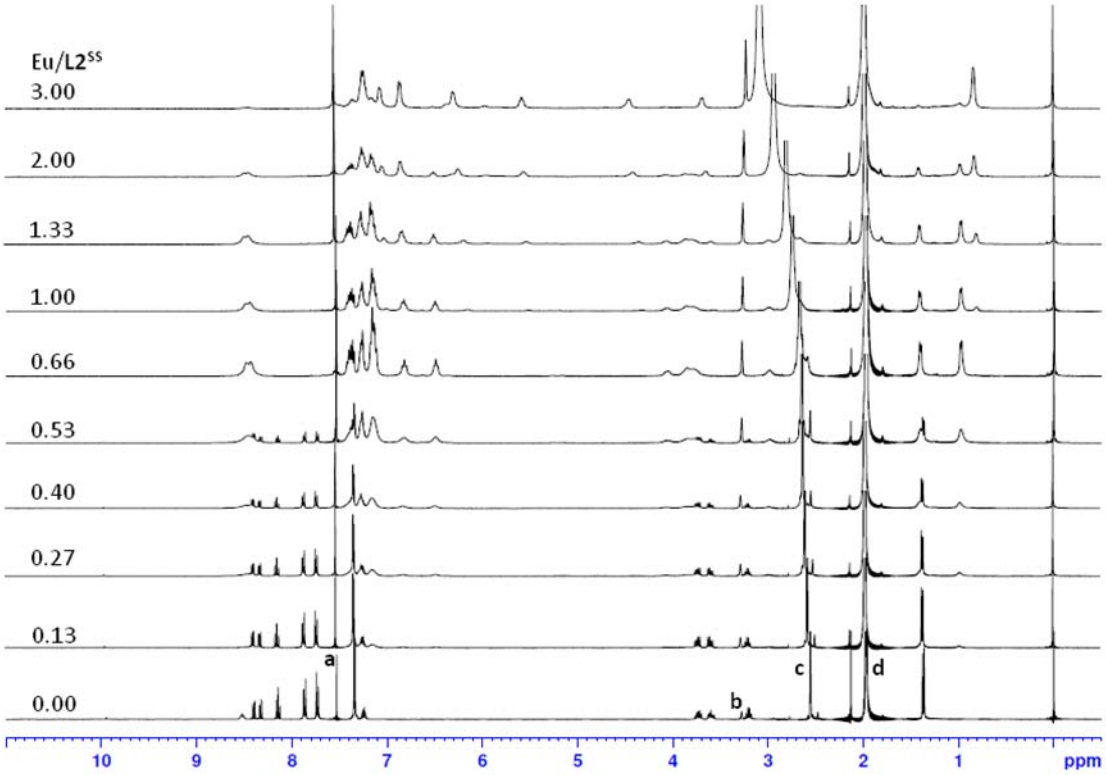

Figure S4. Variation in ^{1}H NMR (400 MHz, 295 K) spectra of titrating **L2^{SS}** (4.64×10^{-3} M in 47:6:47, v/v/v, of $CDCl_3/CD_3OD/CD_3CN$) with $Eu(OTf)_3$ (0.271 M in CD_3OD) at 296K. (Peaks that are marked as a, b, c, d are from the residual solvents.)

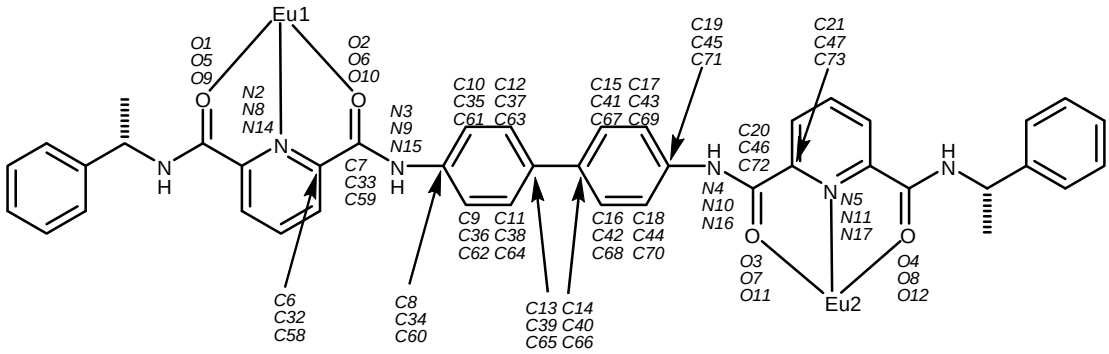

Chart S1. Selected atomic numbering scheme of **[$Eu_2(L1^{SS})_3](CF_3SO_3)_6$** in strand 1(top), 2 (middle), and 3 (bottom) for X-ray crystallography. The corresponding hydrogen atoms, H(number)A, with the same number of the attached carbons are not shown.

Table S1. Selected structural parameters for **[$Eu_2(L1^{SS})_3](CF_3SO_3)_6$**

		Distances(Å)		
	Distance(Å)	Strand 1	Strand 2	Strand 3
Eu(1)–N		N(2), 2.566(5)	N(8), 2.537(5)	N(14), 2.595(5)
Eu(1)–O		O(2), 2.438(5)	O(5), 2.404(5)	O(9), 2.380(5)
Eu(1)–O		O(1), 2.438(5)	O(6), 2.407(5)	O(10), 2.424(4)
Eu(2)–N		N(5), 2.557(6)	N(11), 2.532(5)	N(17), 2.553(5)
Eu(2)–O		O(3), 2.435(4)	O(7), 2.434(4)	O(11), 2.441(5)
Eu(2)–O		O(4), 2.427(5)	O(8), 2.409(5)	O(12), 2.429(5)
Eu(1)–Eu(2)	15.055(1)			

Bite angles			
	angles(°)		angles(°)
O(1)–Eu(1)–N(2)	62.96(17)	O(4)–Eu(2)–N(5)	63.87(17)
O(5)–Eu(1)–N(8)	63.87(18)	O(8)–Eu(2)–N(11)	62.82(16)
O(9)–Eu(1)–N(14)	63.70(16)	O(12)–Eu(2)–N(17)	62.82(18)
N(2)–Eu(1)–O(2)	62.92(16)	N(5)–Eu(2)–O(3)	67.17(18)
N(8)–Eu(1)–O(6)	62.77(17)	N(11)–Eu(2)–O(7)	63.47(16)
N(14)–Eu(1)–O(10)	62.81(16)	N(17)–Eu(2)–O(11)	64.06(17)
O(1)–Eu(1)–O(5)	77.70(16)	O(4)–Eu(2)–O(8)	76.17(17)
O(5)–Eu(1)–O(9)	75.94(16)	O(8)–Eu(2)–O(12)	73.51(16)
O(9)–Eu(1)–O(1)	75.64(16)	O(12)–Eu(2)–O(4)	74.20(16)
N(2)–Eu(1)–N(8)	119.46(17)	N(5)–Eu(2)–N(11)	122.53(18)
N(8)–Eu(1)–N(14)	121.88(17)	N(11)–Eu(2)–N(17)	117.94(17)
N(14)–Eu(1)–N(2)	117.61(15)	N(17)–Eu(2)–N(5)	119.00(18)
O(2)–Eu(1)–O(6)	76.01(16)	O(3)–Eu(2)–O(7)	76.01(14)
O(6)–Eu(1)–O(10)	77.39(15)	O(7)–Eu(2)–O(11)	73.34(15)

O(10)–Eu(1)–O(2)	76.41(16)	O(11)–Eu(2)–O(3)	73.63(15)

Torsional angles					
Strand 1	angles(°)	Strand 2	angles(°)	Strand 3	angles(°)
N(2)–C(6)–C(7)–O(12)	-22.97(103)	N(8)–C(32)–C(33)–O(6)	-19.52(107)	N(14)–C(58)–C(59)–O(10)	-18.38(100)
C(6)–C(7)–N(3)–C(8)	-175.63(70)	C(32)–C(33)–N(9)–C(34)	-171.78(72)	C(58)–C(59)–N(15)–C(60)	-164.52(72)
C(7)–N(3)–C(8)–C(9)	-13.31(135)	C(33)–N(9)–C(34)–C(35)	160.48(77)	C(59)–N(15)–C(60)–C(61)	166.37(76)
C(11)–C(13)–C(14)–C(15)	150.24(75)	C(37)–C(39)–C(40)–C(41)	-44.15(102)	C(63)–C(65)–C(66)–C(67)	-35.42(103)
C(17)–C(19)–N(4)–C(20)	-5.56(126)	C(43)–C(45)–N(10)–C(46)	7.90(115)	C(69)–C(71)–N(16)–C(72)	-8.10(104)
C(19)–N(4)–C(20)–C(21)	-167.72(71)	C(45)–N(10)–C(46)–C(47)	-176.32(69)	C(71)–N(16)–C(72)–C(73)	-167.21(59)
O(3)–C(20)–C(21)–N(5)	-8.27(99)	O(7)–C(46)–C(47)–N(11)	-21.38(103)	O(11)–C(72)–C(73)–N(17)	-17.69(92)

C–H···C	Distance(Å) of (H···C)	Distance(Å) of (C···C)	Angles(°) of (C–H–C)
C38–H38A···C10	2.987(8)	3.800(11)	146.81(51)
C64–H64A···C35	2.874(8)	3.728(11)	153.19(48)
C11–H11A···C61	2.908(8)	3.702(12)	144.23(56)
C67–H67A···C18	2.897(5)	3.788(9)	160.92(48)
C15–H15A···C44	3.154(6)	3.997(10)	151.76(44)
C41–H41A···C70	2.989(9)	3.851(12)	154.92(50)

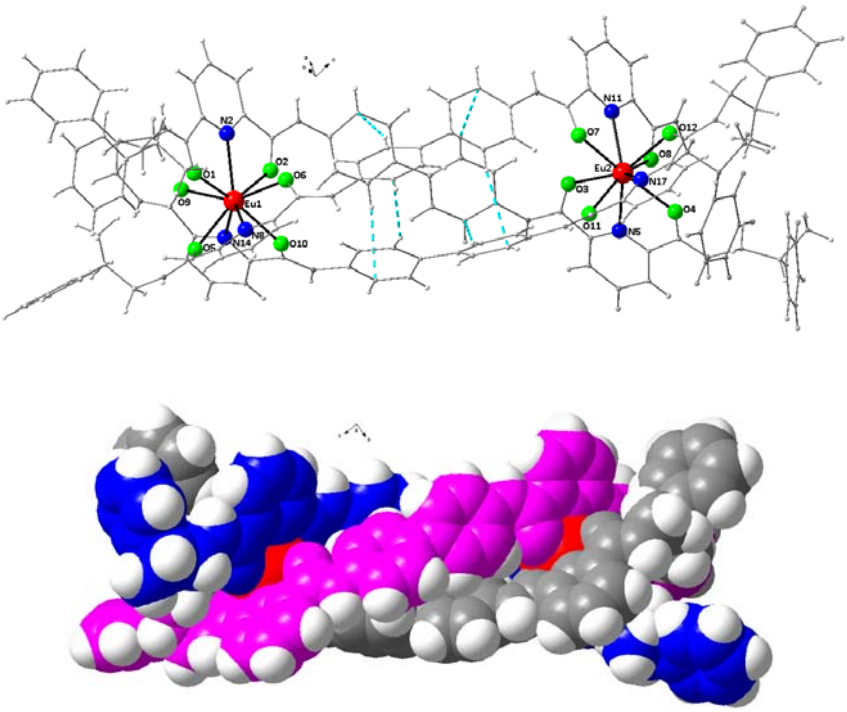

Figure S5. Crystal structure (highlighted only the atoms involving coordination polyhedral; dashed lines indicate CH/π distances < 3.20 Å) and space filling representation of **$[Eu_2(L2^{RR})_3]^{6+}$** showing of helical structure. Disordering of chiral amide side arms occur.

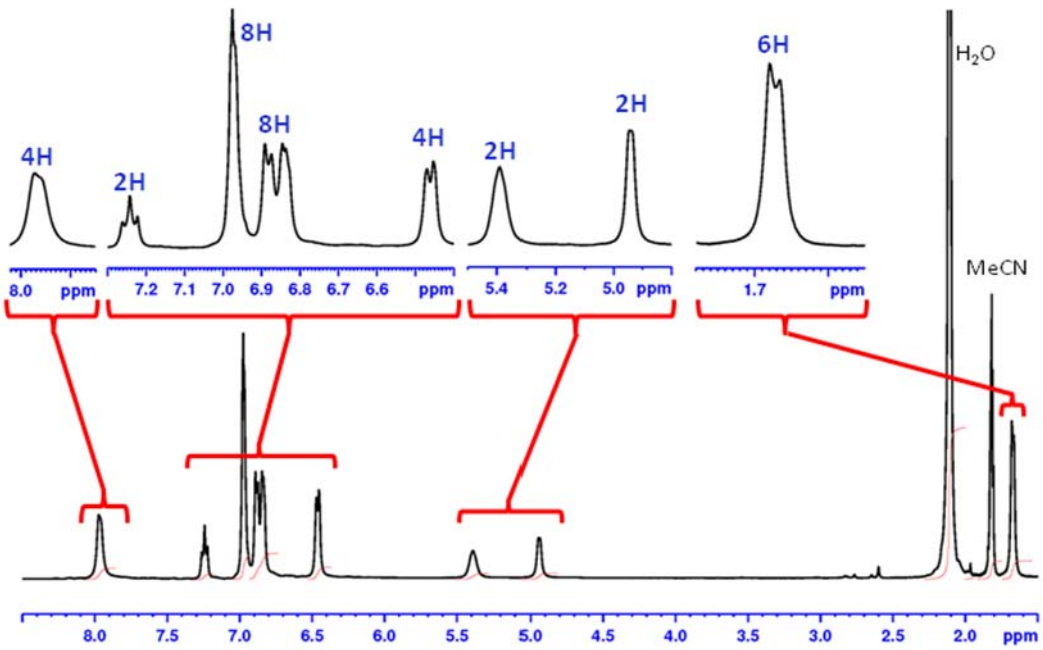

Figure S6. ^{1}H NMR (400 MHz, 298 K) spectrum of **[Eu$_2$(L1^{RR})$_3$](CF$_3$SO$_3$)$_6$** (CD$_3$CN). The insets show the expansion of the corresponding region as indicated.

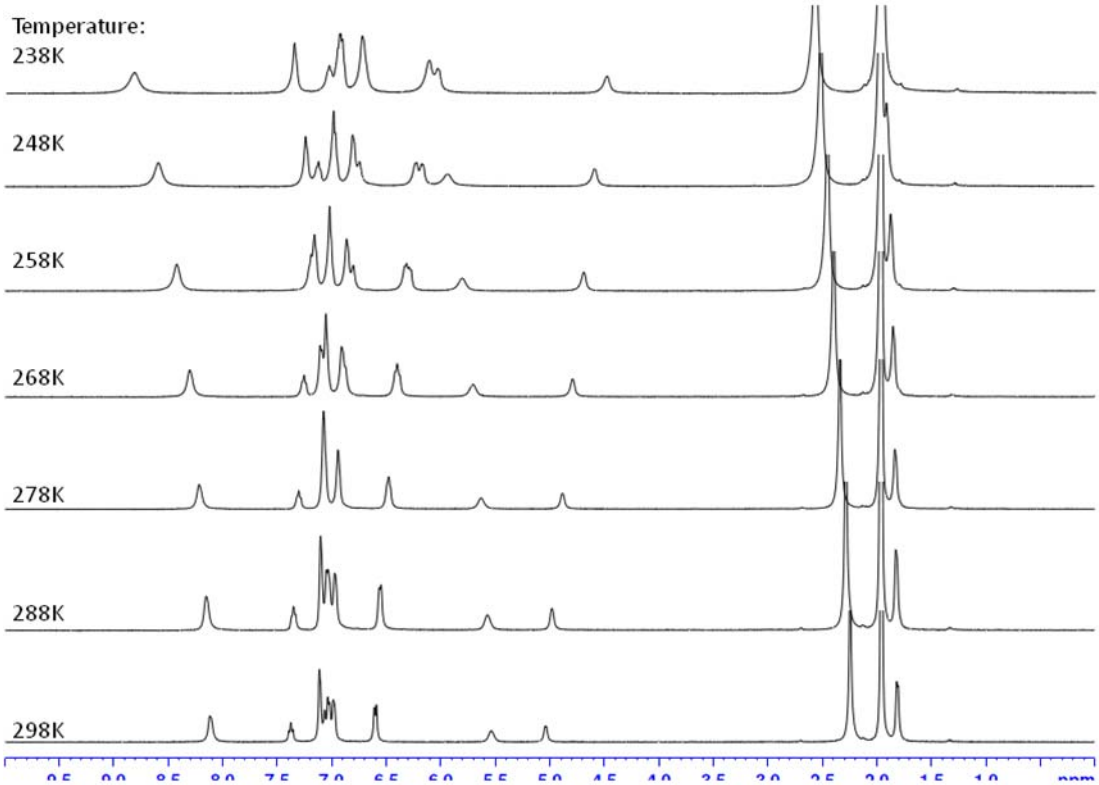

Figure S7. Variable temperature ^{1}H NMR (400 MHz) spectrum of **[Eu$_2$(L1^{SS})$_3$](CF$_3$SO$_3$)$_6$** (CD$_3$CN).

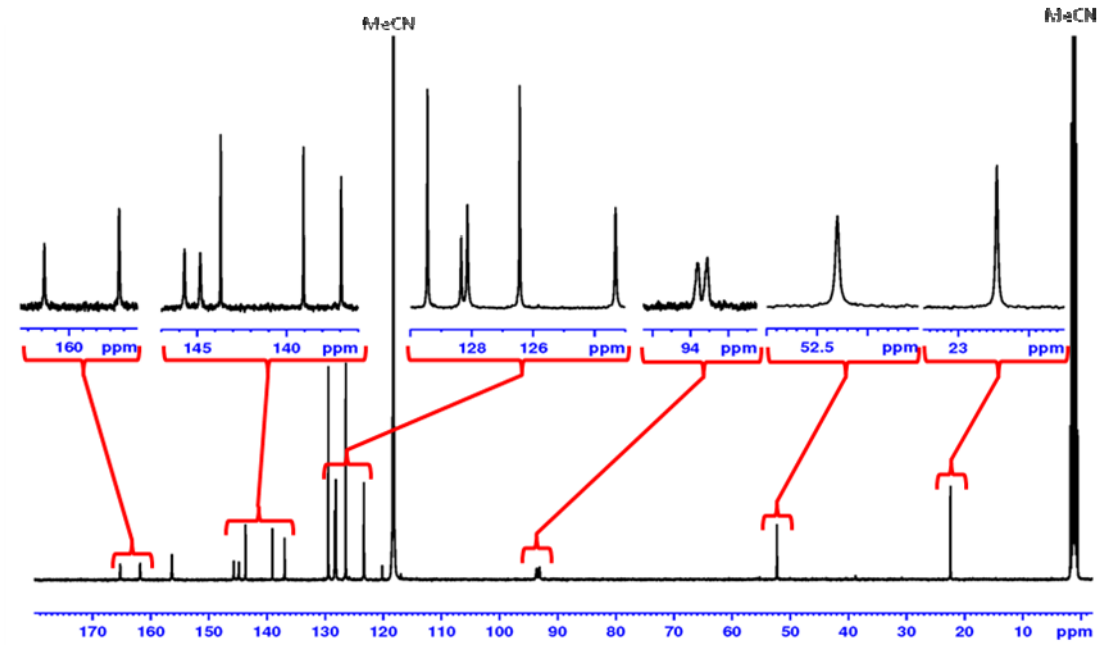

Figure S8. ^{13}C NMR (100.6 MHz, 296 K) spectrum of **[Eu$_2$(L1^{RR})$_3$](CF$_3$SO$_3$)$_6$** (CD$_3$CN). The insets show the expansion of the corresponding region as indicated.

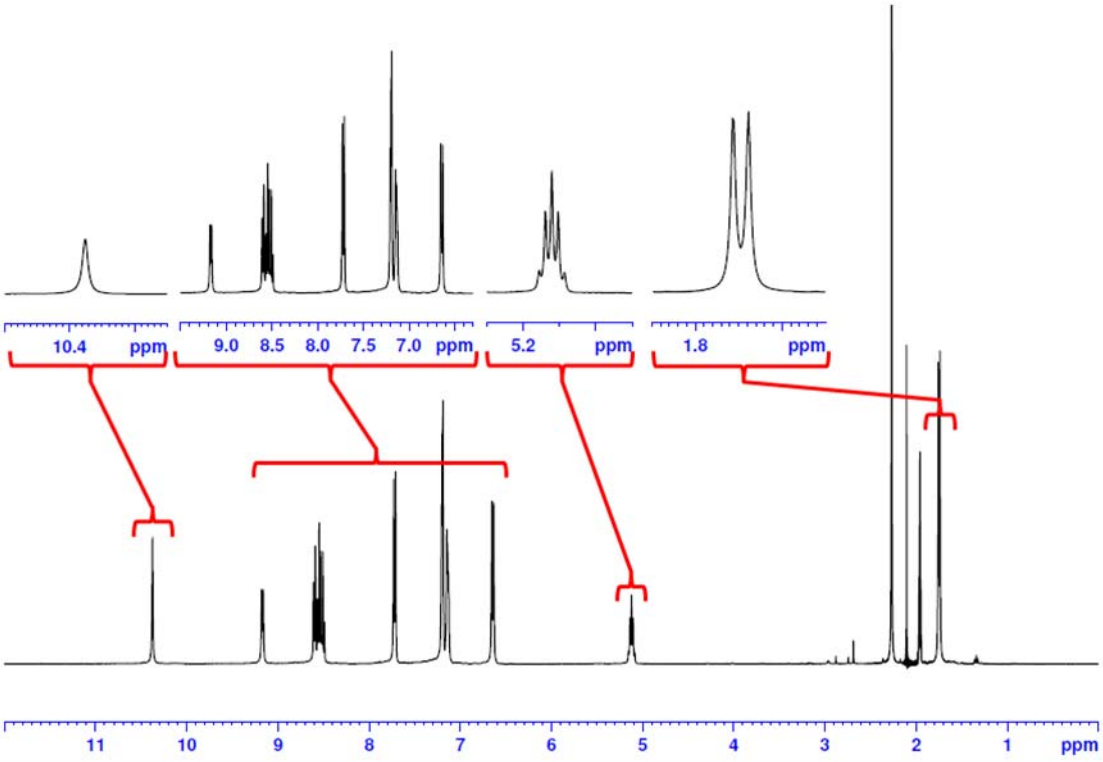

Figure S9. ^{1}H NMR (400 MHz, 298 K) spectrum of **[La$_2$(L1^{SS})$_3$](CF$_3$SO$_3$)$_6$** (CD$_3$CN). The insets show the expansion of the corresponding region as indicated.

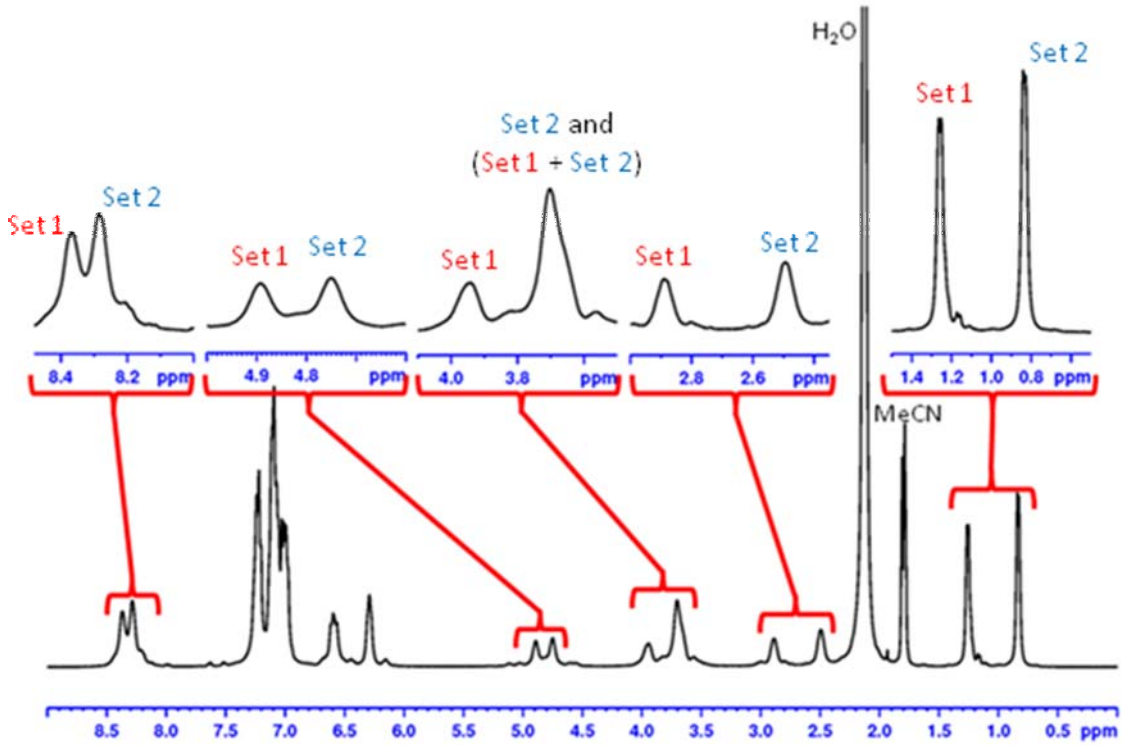

Figure S10. ^{1}H NMR (400 MHz, 298 K) spectrum of **[Eu$_2$(L2^{RR})$_3$](CF$_3$SO$_3$)$_6$** (CD$_3$CN). The insets show the expansion of the corresponding region as indicated. Set 1 and set 2 are preliminary assigned that based on their integration.

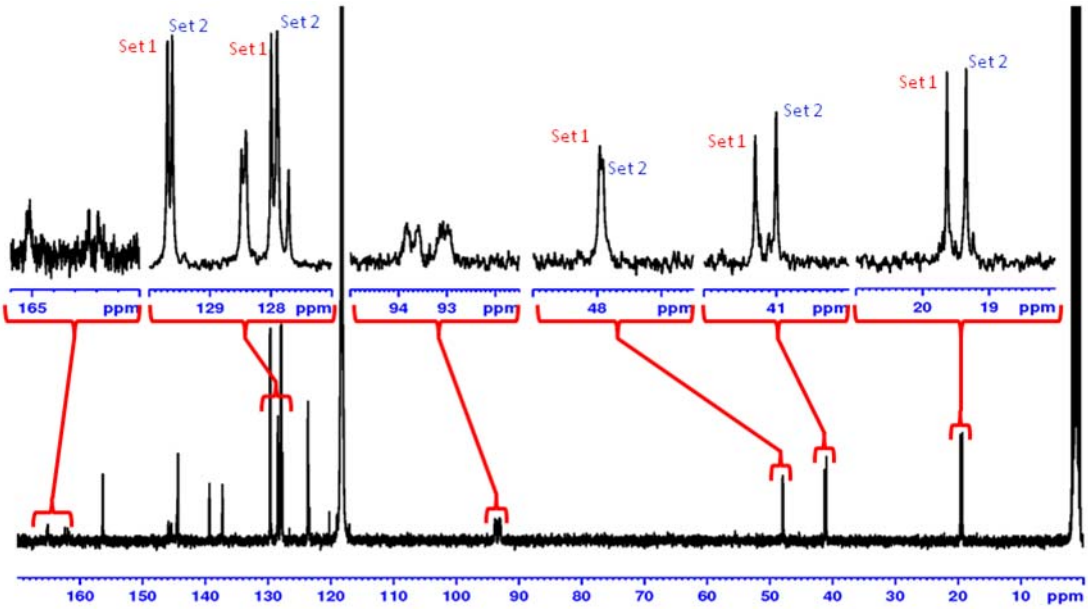

Figure S11. ^{13}C NMR (100.6 MHz, 298 K) spectrum of **[Eu$_2$(L2^{RR})$_3$](CF$_3$SO$_3$)$_6$** (CD$_3$CN). The insets show the expansion of the corresponding region as indicated. Set 1 and set 2 are preliminary assigned that based on their integration.

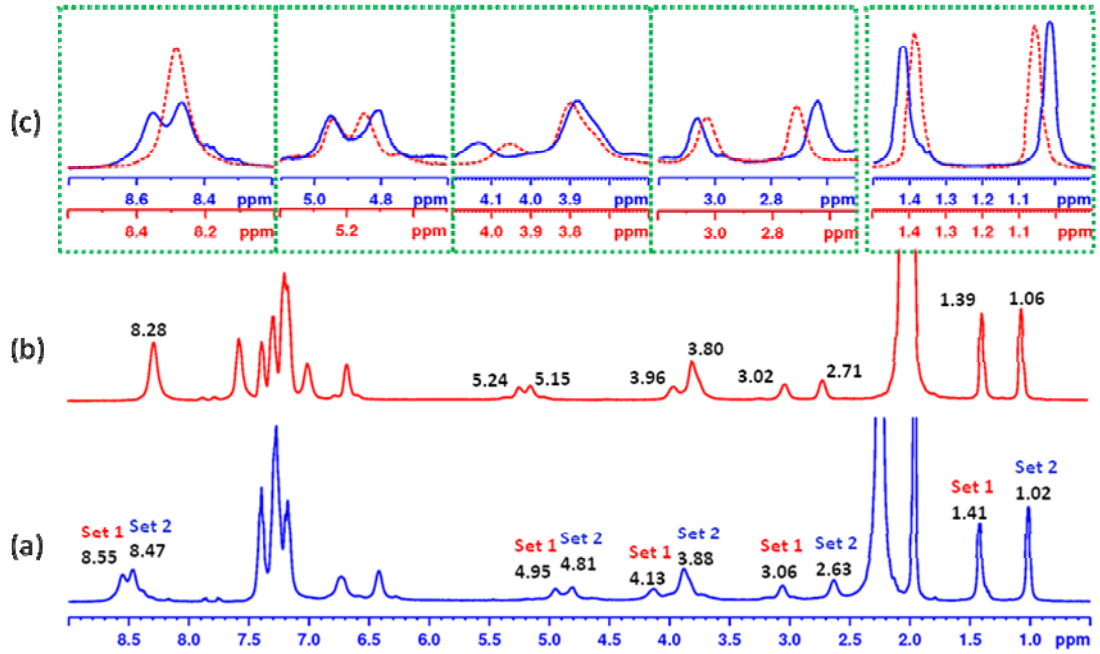

Figure S12. ^{1}H NMR (400 MHz) spectrum of **[Eu$_2$(L2^{RR})$_3$](CF$_3$SO$_3$)$_6$** (CD$_3$CN). a) At 295 K. b) At 345 K, c) Overlaying of the two spectra from 295 K and 345 K.

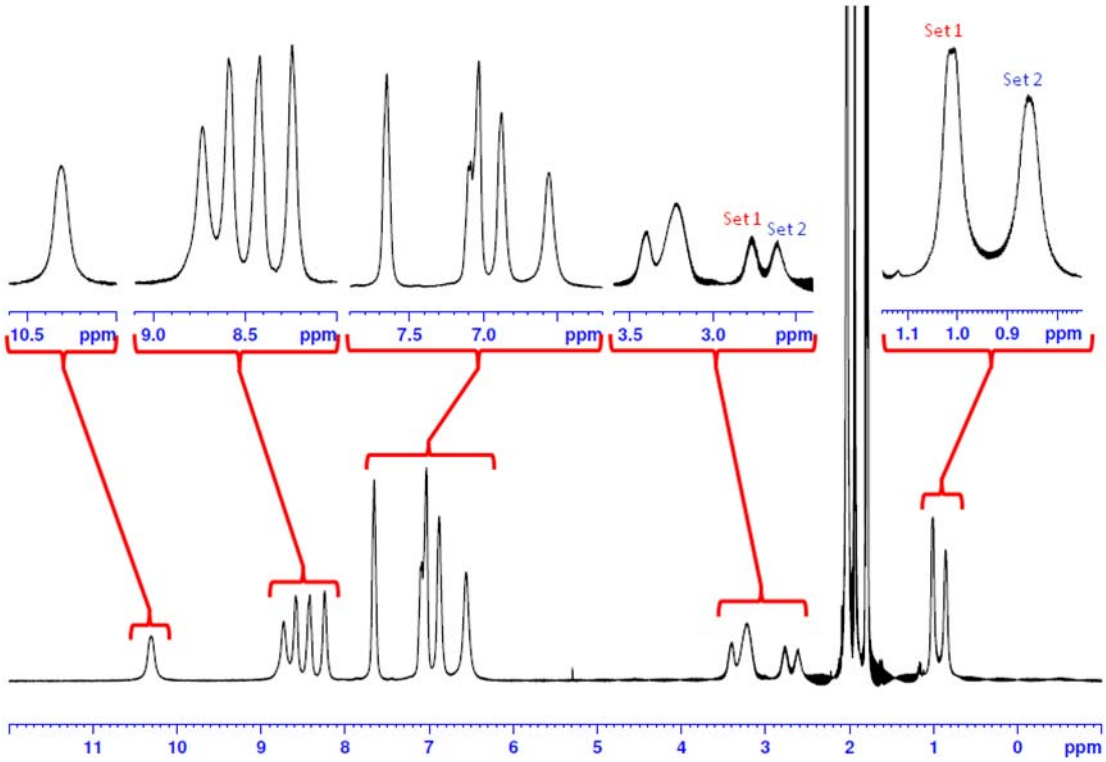

Figure S13. ^{1}H NMR (400 MHz, 298 K) spectrum of **[La$_2$(L2^{SS})$_3$](CF$_3$SO$_3$)$_6$** (CD$_3$CN). The insets show the expansion of the corresponding region as indicated. Set 1 and set 2 are preliminary assigned that based on their integration.

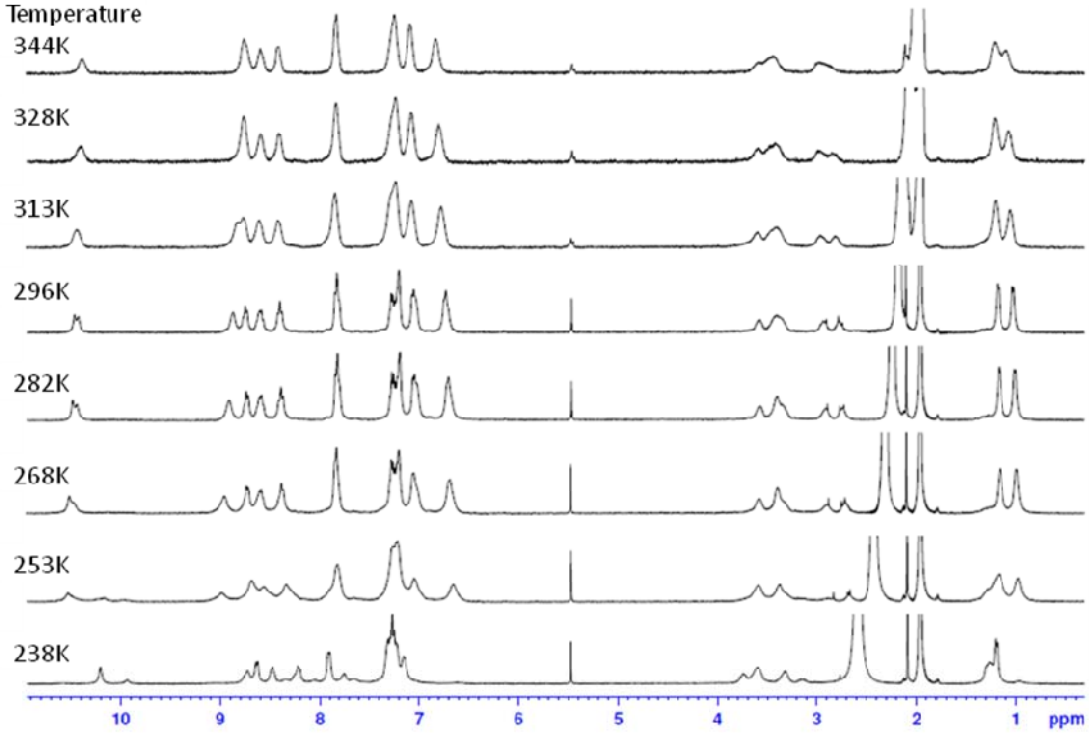

Figure S14. ^{1}H NMR (400 MHz) spectra of **[La$_2$(L2^{SS})$_3$](CF$_3$SO$_3$)$_6$** (CD_3CN) at variable temperature. Another set of peak observed at 253 K and 238 K are due to insolubility of the complex.

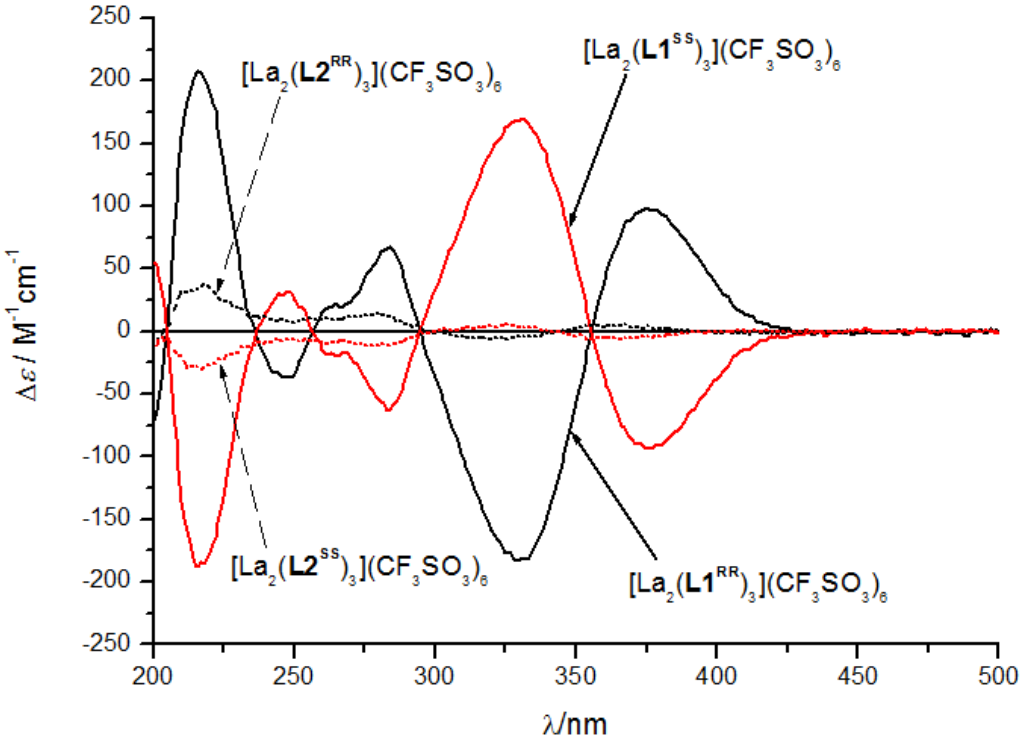

Figure S15. CD spectra of [La$_2$(**L1**)$_3$](CF$_3$SO$_3$)$_6$ (3.58 × 10^{-5} M) and [La$_2$(**L2**)$_3$](CF$_3$SO$_3$)$_6$ (4.23 x 10^{-5} M) in MeCN. Attenuation of 96% (376 nm), 98% (329 nm), 81% (284 nm), 69% (246 nm) and 83% (216 nm) of CD signals are observed.

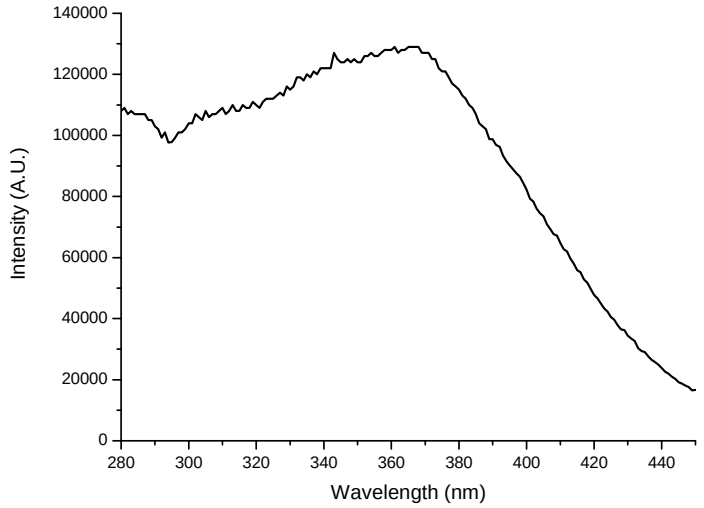

Figure S16. Excitation spectrum of **$[Eu_2(L1^{RR})_3](CF_3SO_3)_6$** (powder, lem = 616 nm, slits = 5-1, filter 455nm).

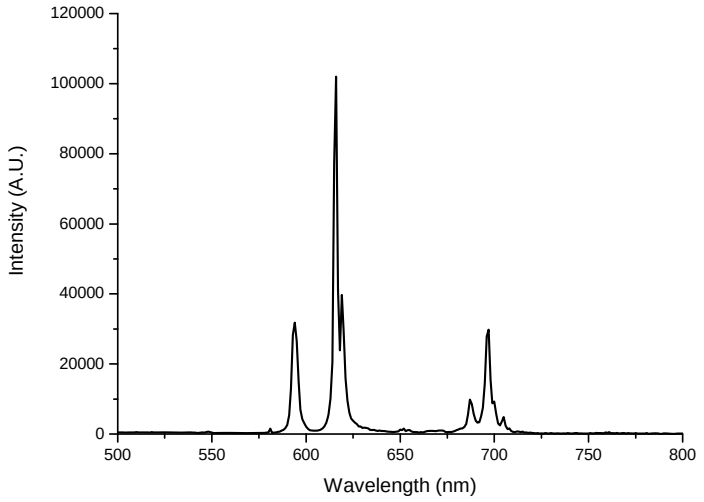

Figure S17. Emission spectrum of **$[Eu_2(L1^{RR})_3](CF_3SO_3)_6$** (powder, lex = 369 nm, slits = 5-1, filter 455nm).

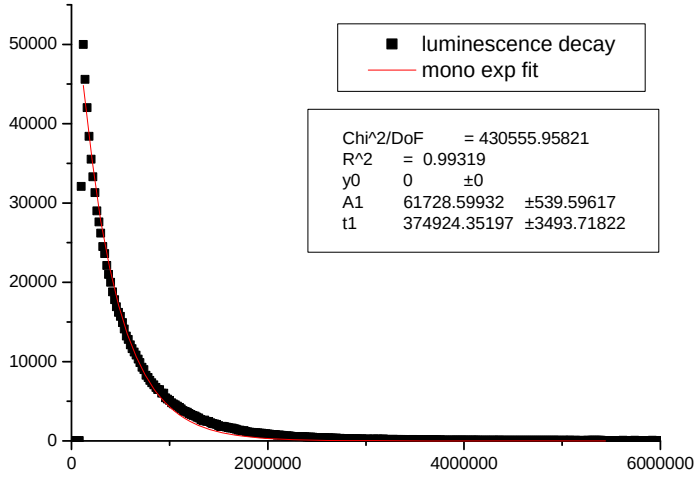

Figure S18. Excited state decay curve and its mono exponential fit of **$Eu_2(L1^{RR})_3](CF_3SO_3)_6$** (powder, lex = 369 nm, slits = 15-3, filter 455nm).

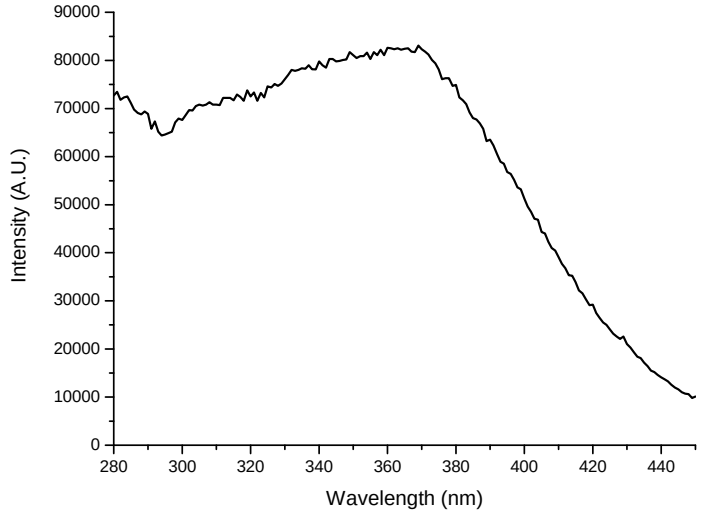

Figure S19. Excitation spectrum of **[$Eu_2(L1^{SS})_3](CF_3SO_3)_6$** (powder, lem = 616 nm, slits = 5-1, filter 455nm).

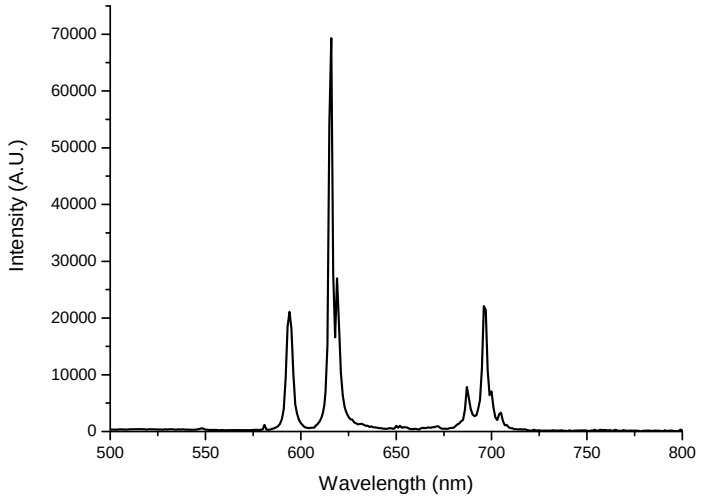

Figure S20. Emission spectrum of **[$Eu_2(L1^{SS})_3](CF_3SO_3)_6$** (powder, lex = 369 nm, slits = 5-1, filter 455nm).

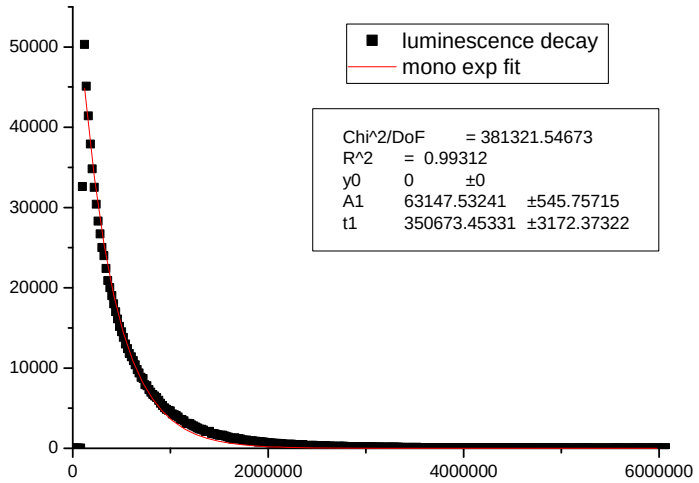

Figure S21. Excited state decay curve and its mono exponential fit of **$[Eu_2(L1^{SS})_3](CF_3SO_3)_6$** (powder, lex = 369 nm, slits = 15-3, filter 455nm).

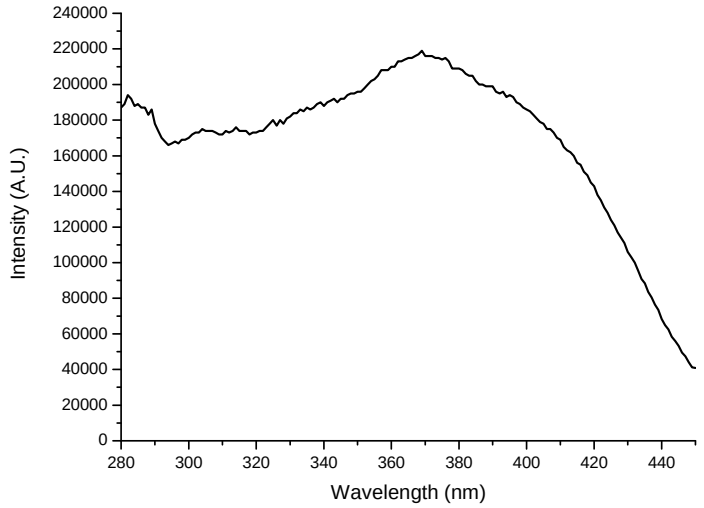

Figure S22. Excitation spectrum of **$[Eu_2(L2^{RR})_3](CF_3SO_3)_6$** (powder, lem = 616 nm, slits = 5-1, filter 455nm).

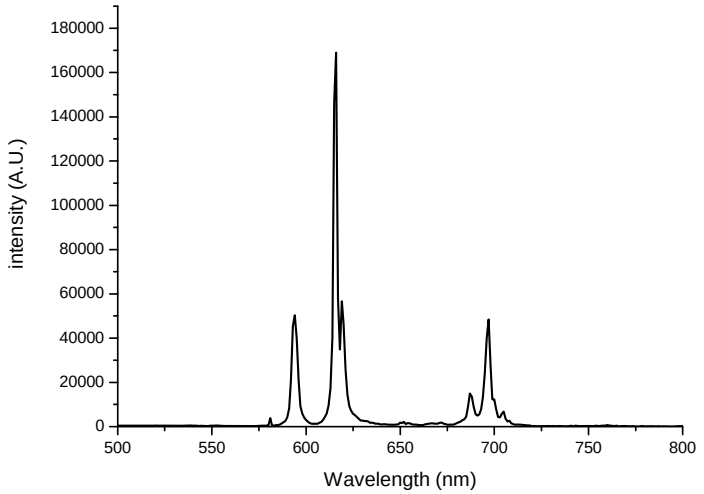

Figure S23. Emission spectrum of **$[Eu_2(L2^{RR})_3](CF_3SO_3)_6$** (powder, lex = 372 nm, slits = 5-1, filter 455nm).

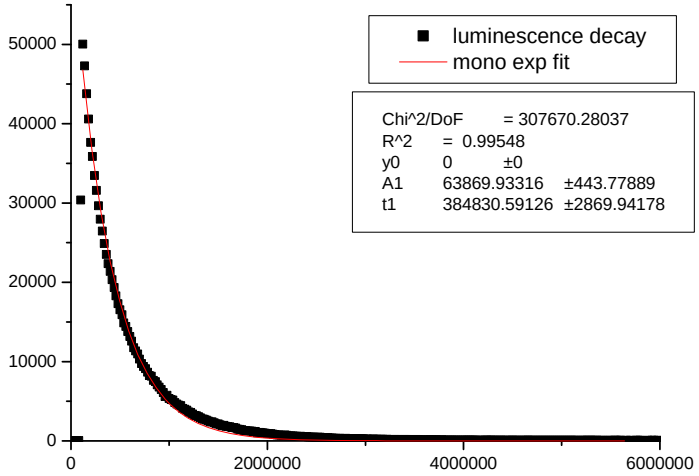

Figure S24. Excited state decay curve and its mono exponential fit of **$[Eu_2(L2^{RR})_3](CF_3SO_3)_6$** (powder, lex = 372 nm, slits = 15-3, filter 455nm).

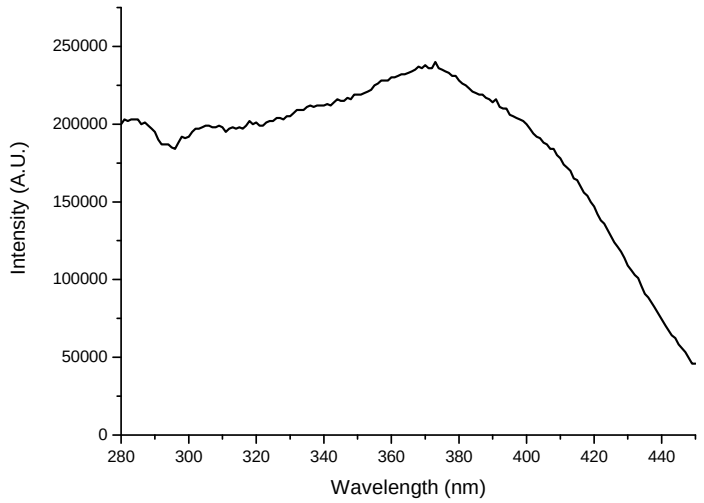

Figure S25. Excitation spectrum of **$[Eu_2(L2^{SS})_3](CF_3SO_3)_6$** (powder, lem = 616 nm, slits = 5-1, filter 455nm).

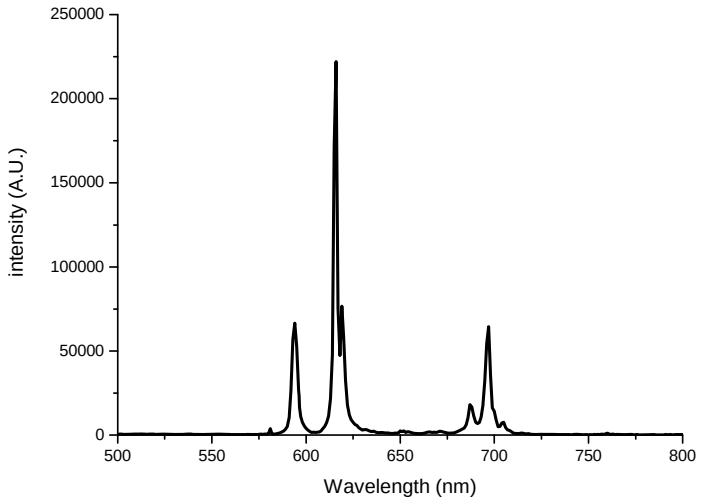

Figure S26. Emission spectrum of **$[Eu_2(L2^{SS})_3](CF_3SO_3)_6$** (powder, lex = 373 nm, slits = 5-1, filter 455nm).

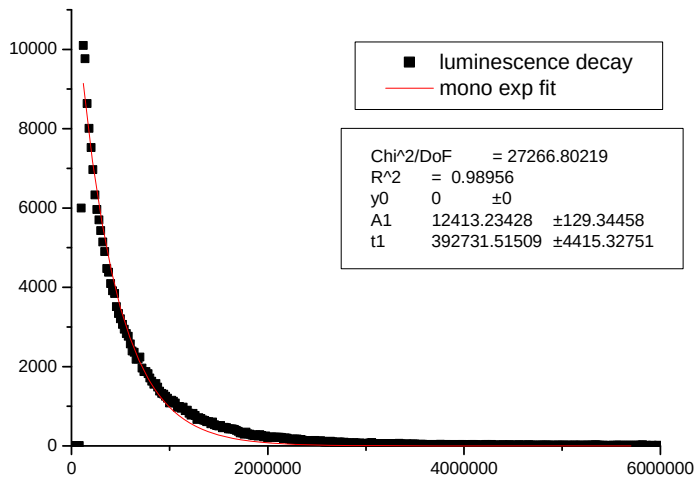

Figure S27. Excited state decay curve and its mono exponential fit of **$[Eu_2(L2^{SS})_3](CF_3SO_3)_6$** (powder, lex = 373 nm, slits = 15-3, filter 455nm).

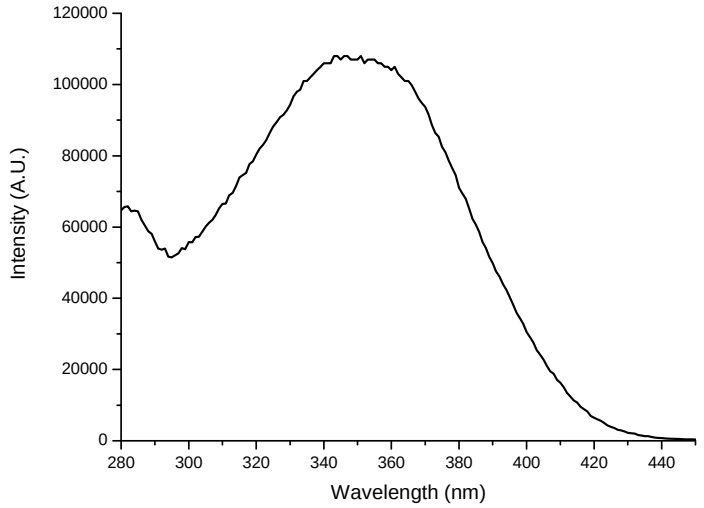

Figure S28. Excitation spectrum of **[$Eu_2(L1^{RR})_3](CF_3SO_3)_6$** (3.23 × 10^{-5} M in MeCN, lem = 616 nm, slits = 5-1, filter 455nm).

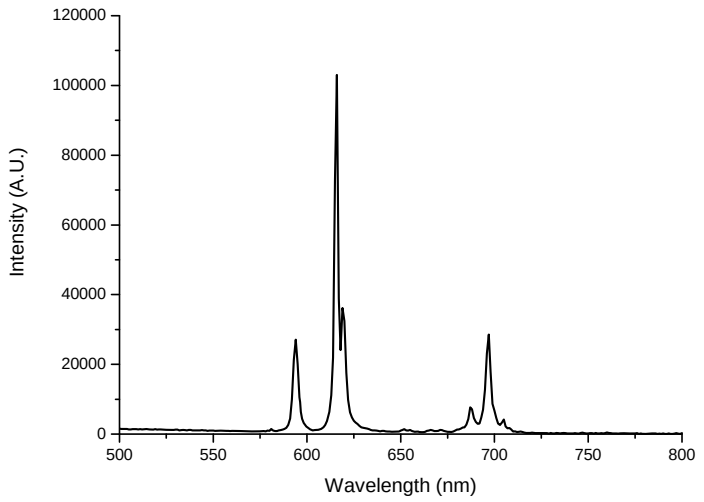

Figure S29. Emission spectrum of **[$Eu_2(L1^{RR})_3](CF_3SO_3)_6$** (3.23 × 10^{-5} M in MeCN, lex = 363 nm, slits = 5-1, filter 455nm).

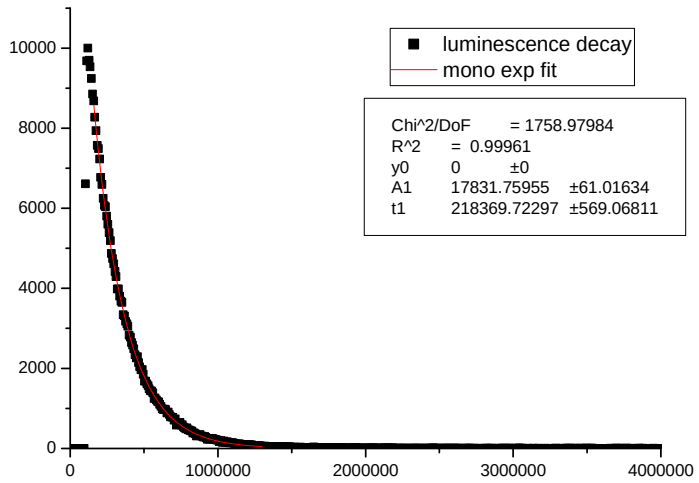

Figure S30. Excited state decay curve and its mono exponential fit of **$[Eu_2(L1^{RR})_3](CF_3SO_3)_6$** ($3.23 \times 10^{-5}$ M in MeCN, lex = 363 nm, slits = 15-3, filter 455nm).

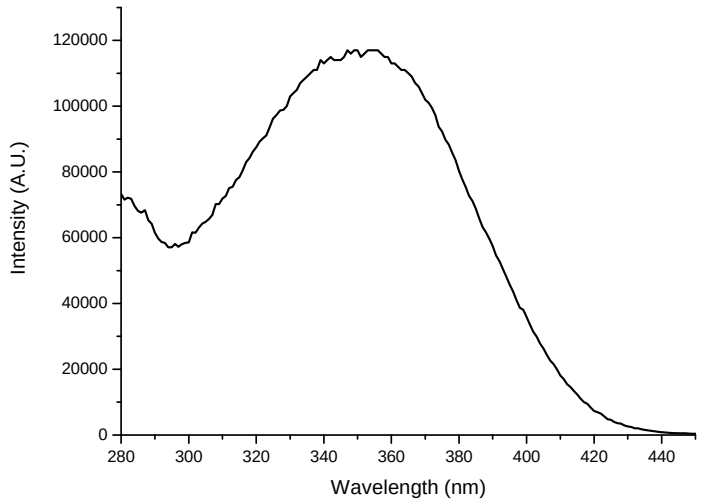

Figure S31. Excitation spectrum of **[$Eu_2(L1^{SS})_3](CF_3SO_3)_6$** (3.23 × 10^{-5} M in MeCN, lem = 616 nm, slits = 5-1, filter 455nm).

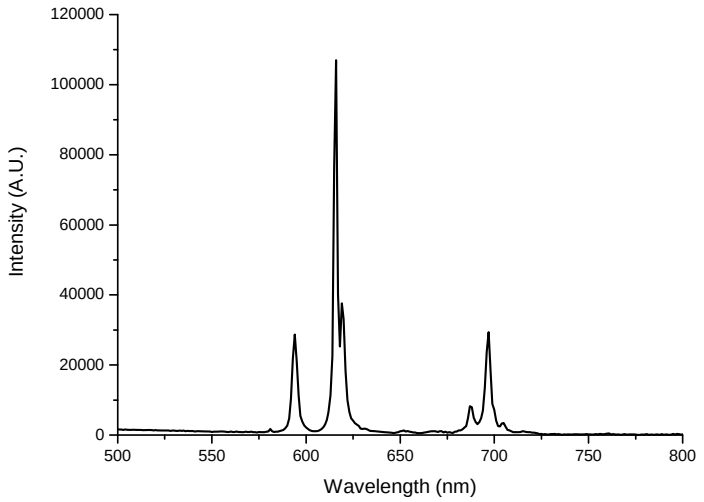

Figure S32. Emission spectrum of **[$Eu_2(L1^{SS})_3](CF_3SO_3)_6$** (3.23 × 10^{-5} M in MeCN, lex = 358 nm, slits = 5-1, filter 455nm).

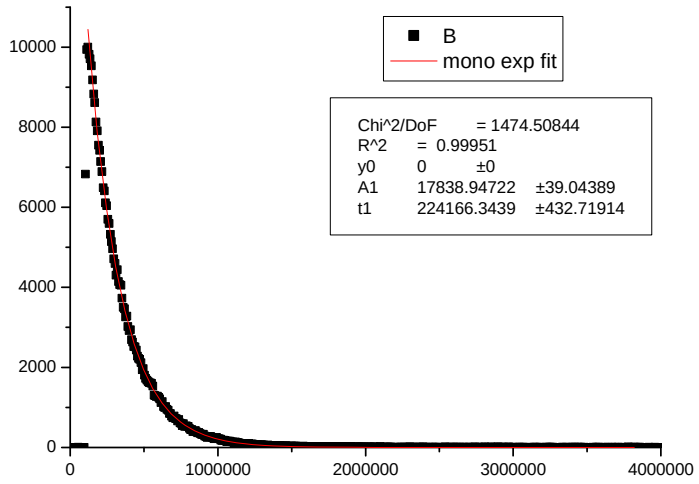

Figure S33. Excited state decay curve and its mono exponential fit of **$[Eu_2(L1^{SS})_3](CF_3SO_3)_6$** ($3.23 \times 10^{-5}$ M in MeCN, lex = 358 nm, slits = 15-3, filter 455nm).

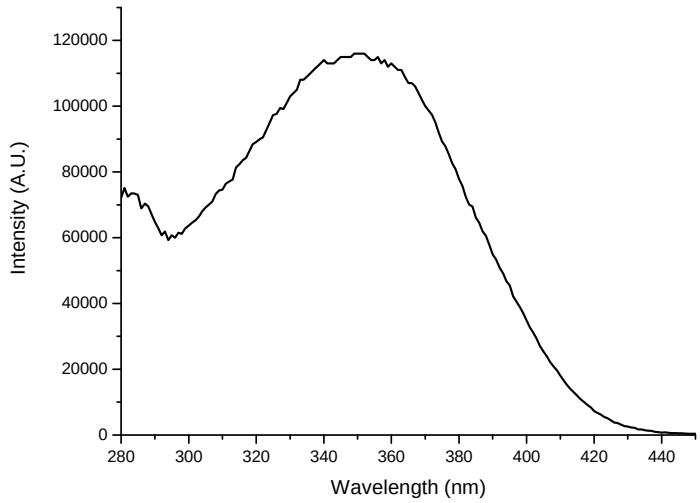

Figure S34. Excitation spectrum of **[$Eu_2(L2^{RR})_3](CF_3SO_3)_6$** (3.47 × 10^{-5} M in MeCN, lem = 616 nm, slits = 5-1, filter 455nm).

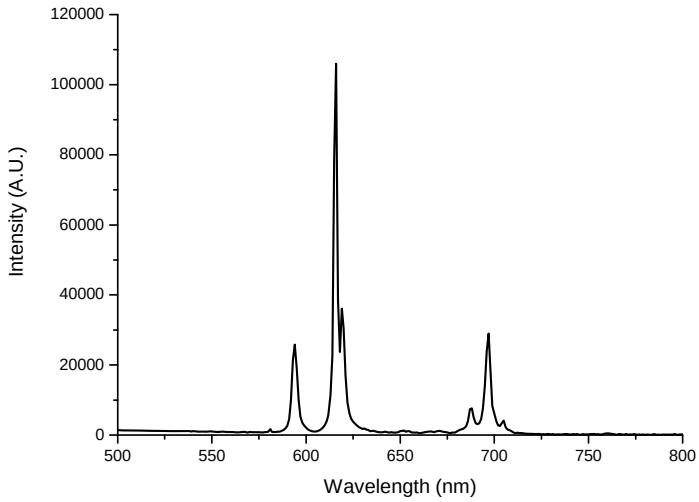

Figure S35. Emission spectrum of **[$Eu_2(L2^{RR})_3](CF_3SO_3)_6$** (3.47 × 10^{-5} M in MeCN, lex = 351 nm, slits = 5-1, filter 455nm).

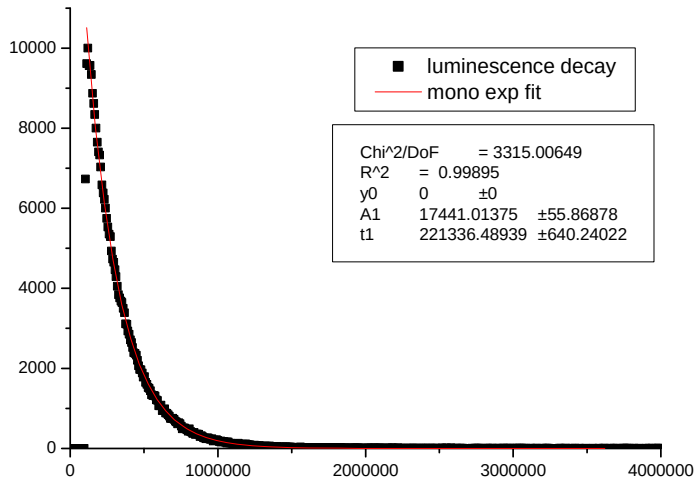

Figure S36. Excited state decay curve and its mono exponential fit of **$[Eu_2(L2^{RR})_3](CF_3SO_3)_6$** (3.47 × 10^{-5} M in MeCN, lex = 351 nm, slits = 15-3, filter 455nm).

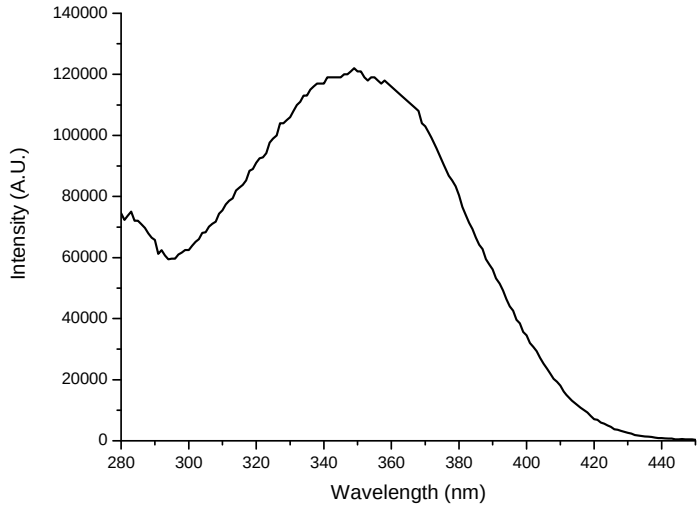

Figure S37. Excitation spectrum of **[$Eu_2(L2^{SS})_3](CF_3SO_3)_6$** (3.15 × 10^{-5} M in MeCN, lem = 616 nm, slits = 5-1, filter 455nm).

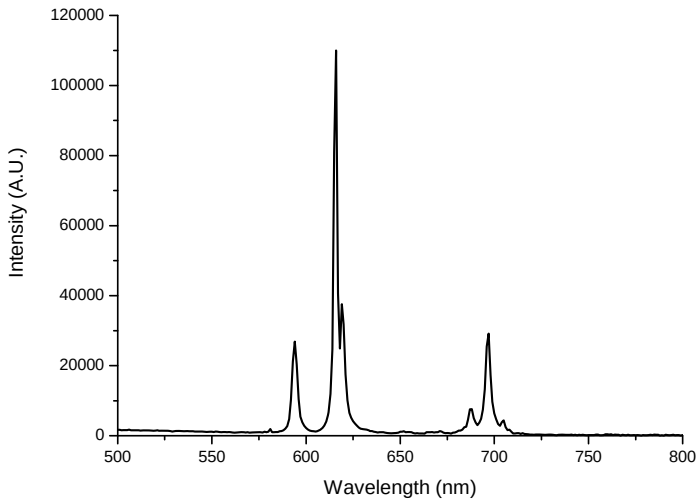

Figure S38. Emission spectrum of **[$Eu_2(L2^{SS})_3](CF_3SO_3)_6$** (3.15 × 10^{-5} M in MeCN, lex = 351 nm, slits = 5-1, filter 455nm).

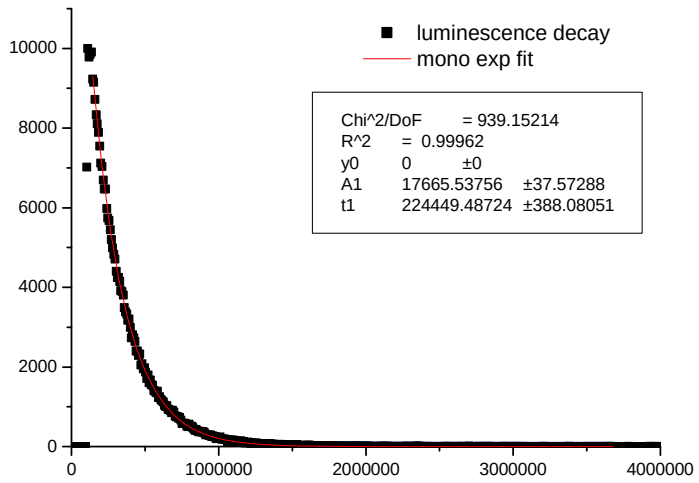

Figure S39. Excited state decay curve and its mono exponential fit of **$[Eu_2(L2^{SS})_3](CF_3SO_3)_6$** ($3.15 \times 10^{-5}$ M in MeCN, lex = 351 nm, slits = 15-3, filter 455nm).

Table S2. A summary of selected photophysical properties, UV-Vis absorption and luminescence data, of **$[Eu_2(L)_3](CF_3SO_3)_6$** in acetonitrile solution[a]

	λ_{abs}^{max} (nm)	ε^{max} ($L \cdot mol^{-1} \cdot cm^{-1}$)	λ_{em}^{max} (nm)	τ (ms)
$[Eu_2(L1^{RR})_3](CF_3SO_3)_6$	340	102300	616	0.22
$[Eu_2(L1^{SS})_3](CF_3SO_3)_6$	340	107000	616	0.22
$[Eu_2(L2^{RR})_3](CF_3SO_3)_6$	340	99000	616	0.22
$[Eu_2(L2^{SS})_3](CF_3SO_3)_6$	340	98000	616	0.22
$[La_2(L1^{SS})_3](CF_3SO_3)_6$	338	103000	449[b]	0.014[b]

[a]Using a 1mm cuvette and filter 455 nm. [b]Measurement performed at 77 K in 1:4 of MeOH/EtOH and using a 10 mm cuvette.

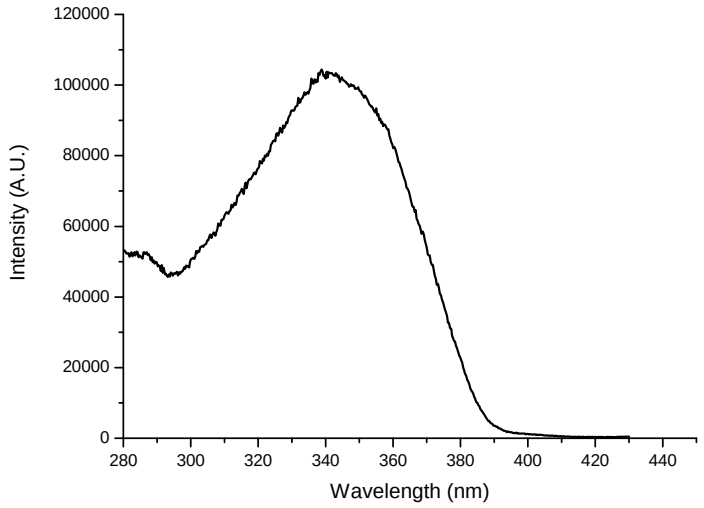

Figure S40. Excitation spectrum of **[$Gd_2(L1^{SS})_3](CF_3SO_3)_6$** (2.88 × 10^{-6} M in 1:4, v/v of MeOH/EtOH at 77K, lem = 450 nm, slits = 5-1).

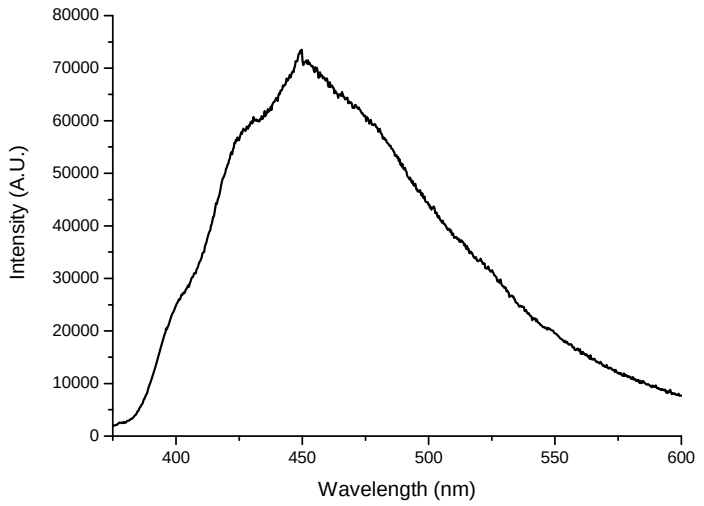

Figure S41. Emission spectrum of **[$Gd_2(L1^{SS})_3](CF_3SO_3)_6$** (2.88 × 10^{-6} M in 1:4 of MeOH/EtOH at 77K, lex = 340 nm, slits = 5-1).

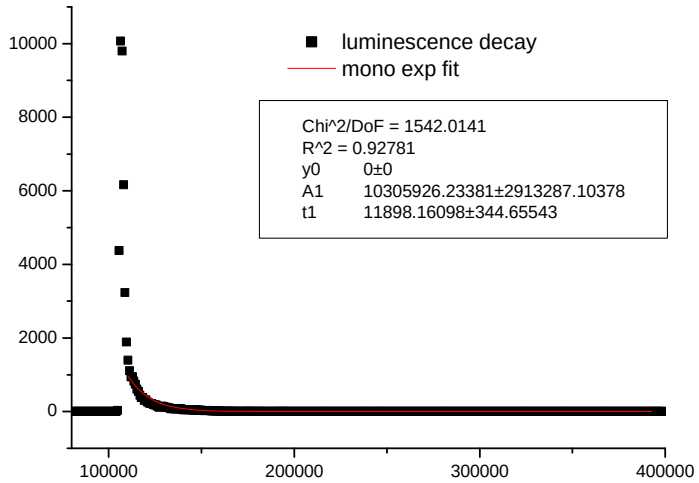

Figure S42. Excited state decay curve and its mono exponential fit of **$[Gd_2(L1^{SS})_3](CF_3SO_3)_6$** ($2.88 \times 10^{-6}$ M in 1:4 of MeOH/EtOH at 77K, lex = 340 nm, slits = 15-3).

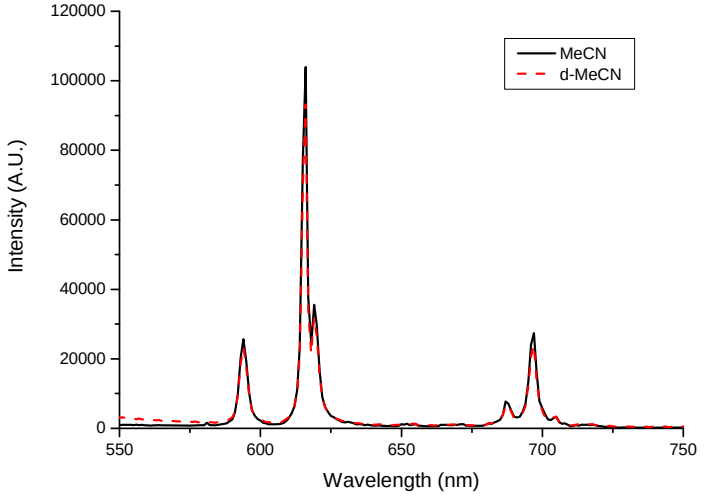

Figure S43. Emission spectrum of **[$Eu_2(L2^{RR})_3](CF_3SO_3)_6$** (3.15 × 10^{-5} M in MeCN or d-MeCN, lex = 351 nm, slits = 5-1, filter 455nm).

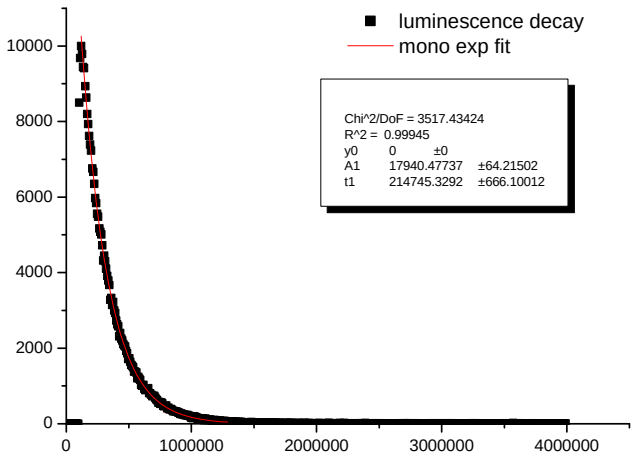

Figure S44. Excited state decay curve and its mono exponential fit of **[$Eu_2(L2^{RR})_3](CF_3SO_3)_6$** (3.15 × 10^{-5} M in d-MeCN, lex = 351 nm, slits = 15-3, filter 455nm).

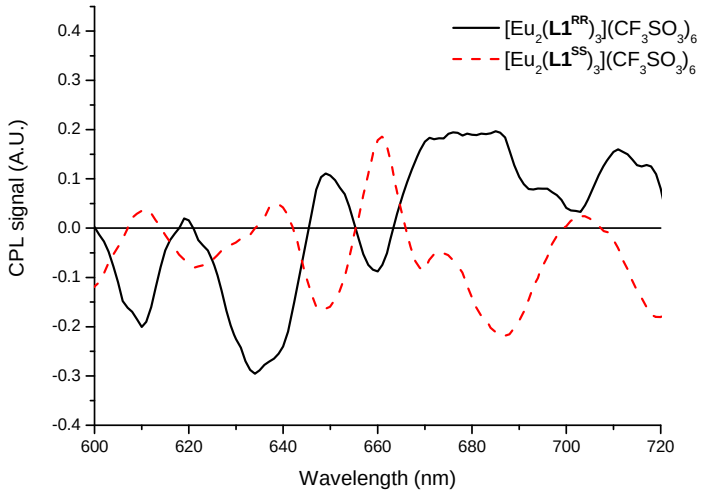

Figure S45. Preliminary results of CPL for $[Eu_2(\mathbf{L1})_3](CF_3SO_3)_6$ (2.30 × 10^{-3} M, 10 mm cuvette, MeCN).[5]

Table S3. Crystal data and structure refinement of **$[Eu_2(L1^{SS})_3](CF_3SO_3)_6$**, **$[Eu_2(L2^{RR})_3](CF_3SO_3)_6$**, and **$L2^{RR}$**

	$[Eu_2(L1^{SS})_3](CF_3SO_3)_6$,	**$[Eu_2(L2^{RR})_3](CF_3SO_3)_6$**	**$L2^{RR}$**
Empirical formula	$C_{126}H_{108}Eu_2N_{18}O_{12}$	$C_{132}H_{120}Eu_2N_{18}O_{12}$	$C_{44}H_{40}N_6O_4$
Formula weight	2370.22	2454.38	716.82
Temperature	296(2) K	296(2) K	296(2) K
Wavelength	0.71073 Å	0.71073 Å	0.71073 Å
Crystal system, space group	Orthorhombic, *P* 2_1 2_1 2	Triclinic, *P*-1	Monoclinic, *P* 2_1
Unit cell dimensions	a = 26.0606(10), b = 28.4219(9), c = 23.3299(9), α = β = γ = 90	a = 16.6790(5), b = 20.3099(6), c = 24.4218(8), α = 87.025(2), β = 70.961(2), γ = 89.269(2)	a = 10.3285(6), b = 17.8133(12), c = 10.5822(7), α = 90, β = 100.506(4) α = 90
Volume	17280.3(11) $Å^3$	7809.7(4) $Å^3$	1914.3(2) $Å^3$
Z, Calculated density	4, 0.911 mg/m^3	2, 1.044 mg/m^3	2, 1.244 mg/m^3
Absorption coefficient	0.765 mm^{-1}	0.849 mm^{-1}	0.081 mm^{-1}
F(000)	4848	2520	756
Crystal size	0.20 x 0.46 x 0.48 mm	0.04 x 0.16 x 0.24 mm	0.04 x 0.36 x 0.56 mm

θ range for data collection	2.60 to 25.35 deg	2.58 to 26.37 deg	2.78 to 24.71 deg
Limiting indices	$-31 \le h \le 24$, $-34 \le k \le 34$, $-28 \le l \le 28$	$-20 \le h \le 20$, $-25 \le k \le 25$, $-30 \le l \le 30$	$-12 \le h \le 12$, $-20 \le k \le 20$, $-12 \le l \le 12$
Reflections collected / unique	144075/31600	196288/31901	23536 / 6477
Absorption correction	Semi-empirical from equivalents	Semi-empirical from equivalents	Semi-empirical from equivalents
Refinement method	Full-matrix least-squares on F^2	Full-matrix least-squares on F^2	Full-matrix least-squares on F^2
Data/restraints/ parameters	31600 / 0 / 1261	31901 / 6 / 1161	6477 / 2 / 487
Goodness-of-fit on F^2	1.010	0.952	1.021
Final R indices [I>2σ(I)]	R_1 = 0.0607, wR_2 = 0.0986	R_1 = 0.0743, wR_2 = 0.1956	R_1 = 0.0583, wR_2 = 0.1407
R indices (all data)	R_1 = 0.1062, wR_2 = 0.1073	R_1 = 0.1465, wR_2 = 0.2181	R_1 = 0.1163, wR_2 = 0.1712
Flack parameter	0.018(8)	N/A	0(2)
Extinction coefficient	N/A	N/A	0.0054(14)
Largest diff. peak and hole	0.749 and -0.355 $Å^{-3}$	1.034 and -0.622 $Å^{-3}$	0.253 and -0.193 $Å^{-3}$

Note: All data were collected at ambient temperature. **$[Eu_2(L1^{SS})_3](CF_3SO_3)_6$**, and **$[Eu_2(L2^{RR})_3](CF_3SO_3)_6$** were refined using PLATON/SQUEEZE, as such parameters such as empirical formula, formula weight, calculated density, etc. only reflect the refined structure as is.

References:

1. Bruker (2001). *SADABS*. Bruker AXS Inc., Madison, Wisconsin, USA.
2. Bruker (2007). *APEX2* and *SAINT*. Bruker AXS Inc., Madison, Wisconsin, USA.
3. (and 10) Sheldrick, G. M. (2008). *Acta Cryst.* A**64**, 112-122.
4. Spek A. L. (2009) *Acta Cryst.* D**65**, 148-155.
5. CPL experiments were helped by Mr Chi-Fai Chan and Dr. Ka-Leung Wong in department of chemistry, hong kong baptist university, HK SAR.

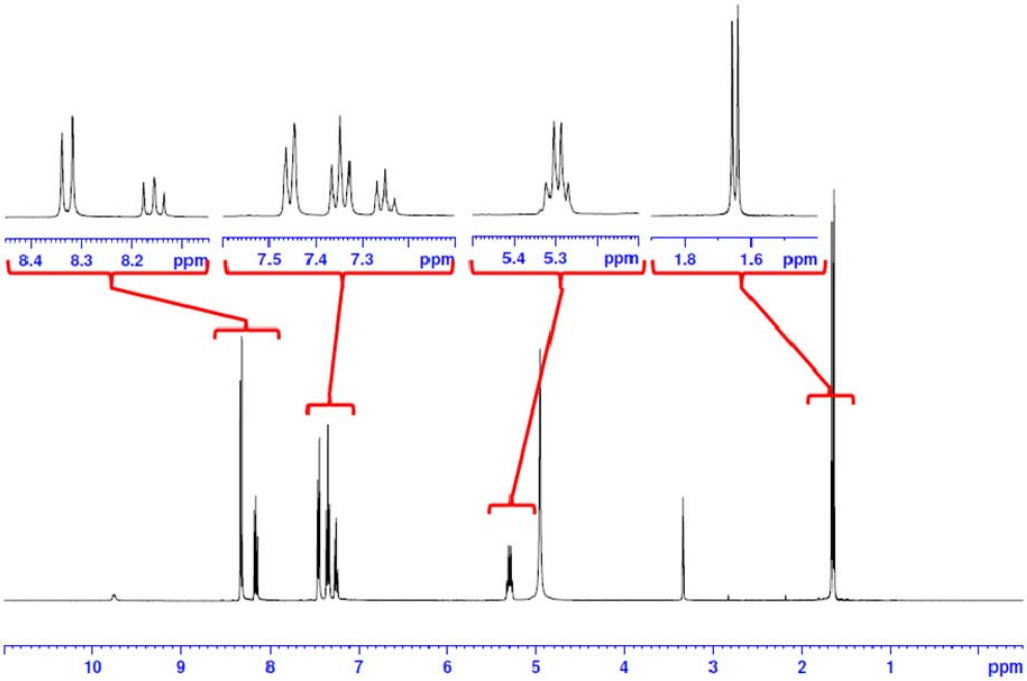

Figure S46. ^{1}H NMR spectrum of **1^{S}** in CD_3OD. The insets show the expansion of the corresponding region as indicated.

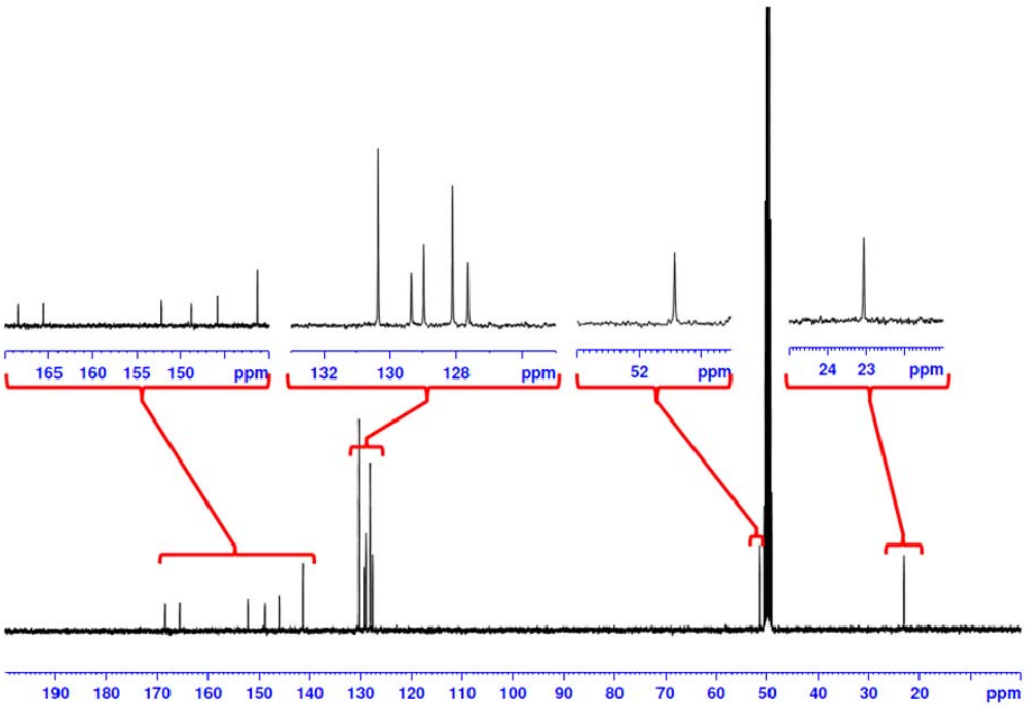

Figure S47. ^{13}C NMR spectrum of **1^{S}** in CD_3OD. The insets show the expansion of the corresponding region as indicated.

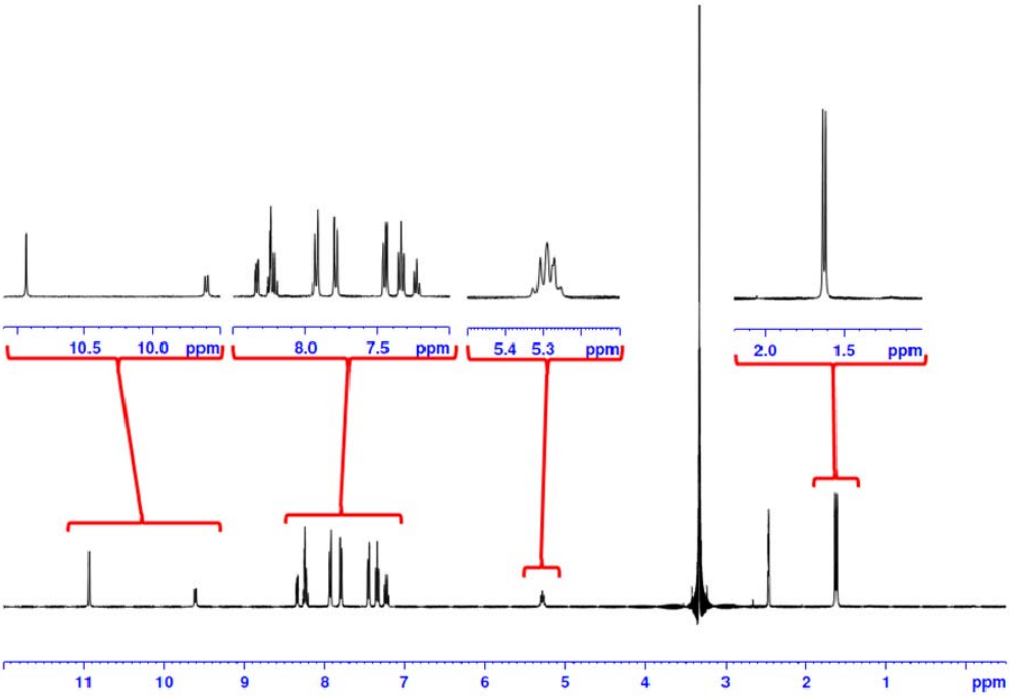

Figure S48. ^{1}H NMR spectrum of **L1^{RR}** in $(CD_3)_2SO$. The insets show the expansion of the corresponding region as indicated.

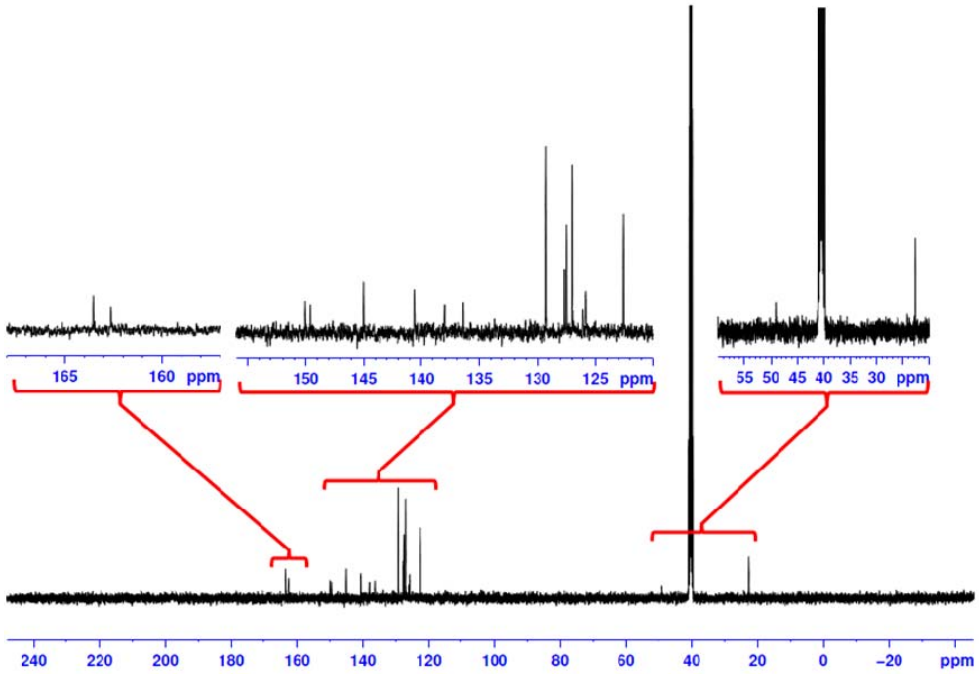

Figure S49. ^{13}C NMR spectrum of **L1^{RR}** in $(CD_3)_2SO$. The insets show the expansion of the corresponding region as indicated.

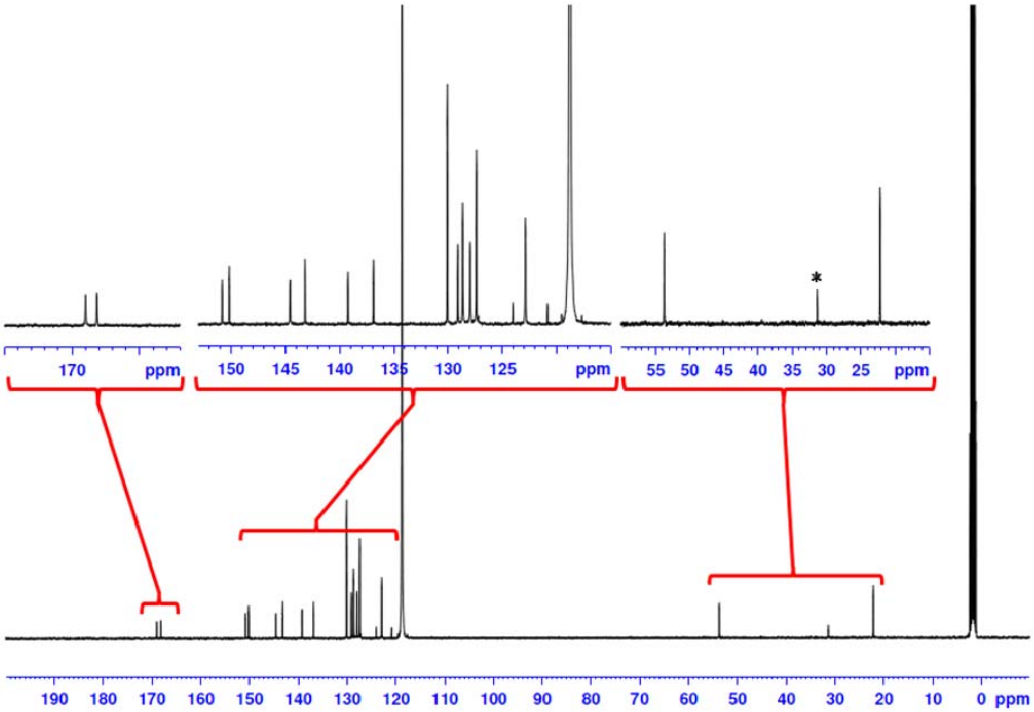

Figure S50. ^{13}C NMR spectrum of **[La$_2$(L1^{SS})$_3$](CF$_3$SO$_3$)$_6$** in CD_3CN. The insets show the expansion of the corresponding region as indicated. The chemical shift with an asteroid is not very clear. It was shown to correlate a chemical shift at 2.10 ppm (singlet) in the corresponding ^{1}H NMR spectrum in HSQC experiment.

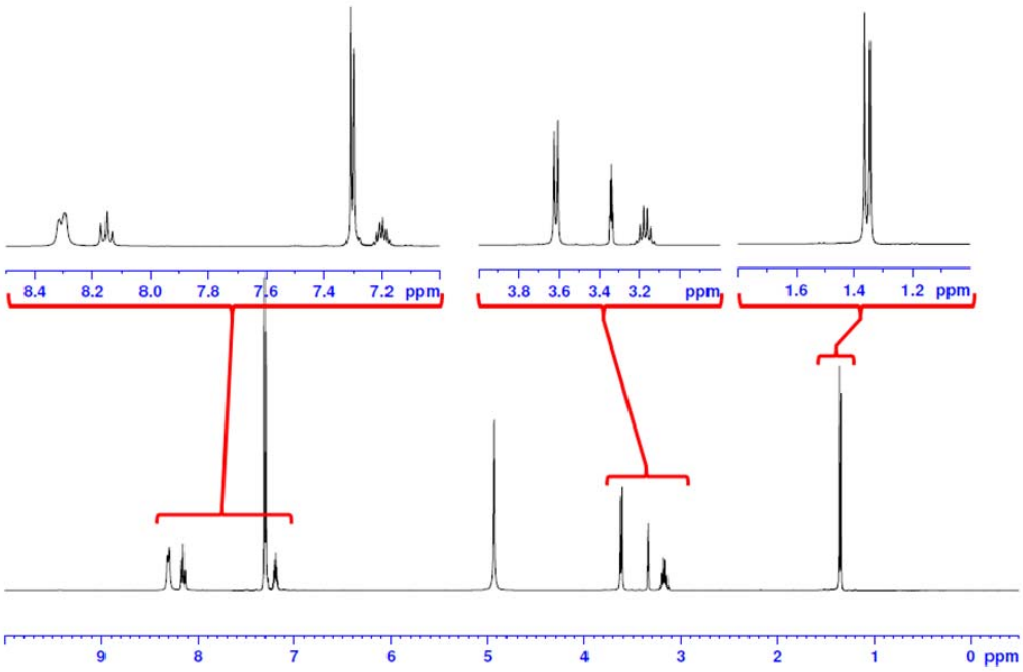

Figure S51. ^{1}H NMR spectrum of **2^S** in CD_3OD. The insets show the expansion of the corresponding region as indicated.

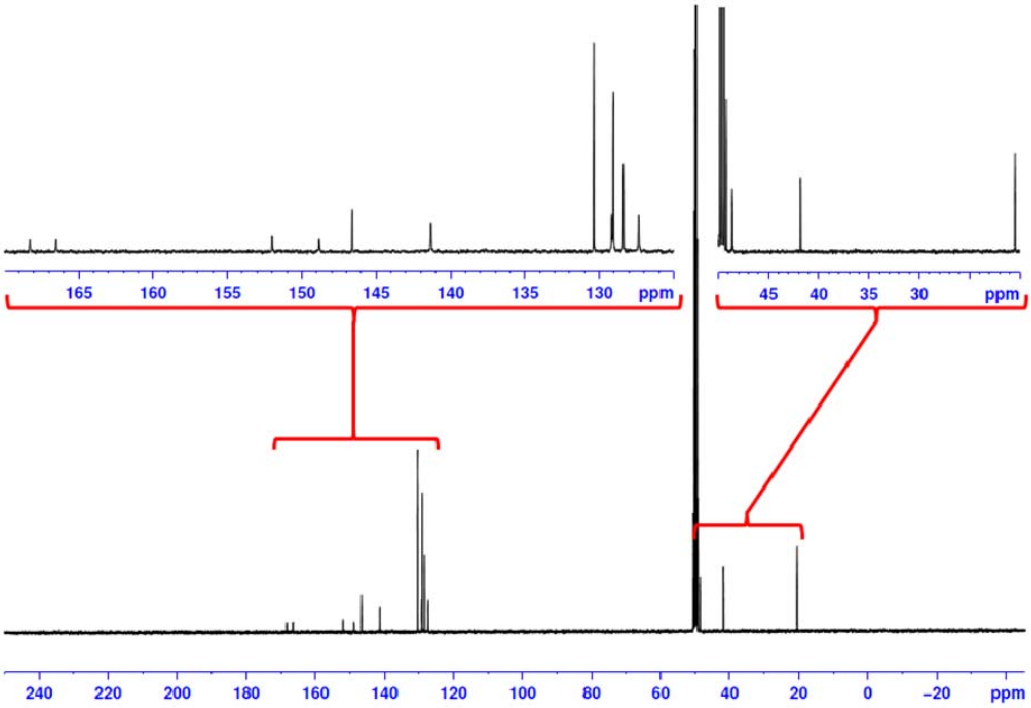

Figure S52. ^{13}C NMR spectrum of **2^{S}** in CD_3OD. The insets show the expansion of the corresponding region as indicated.

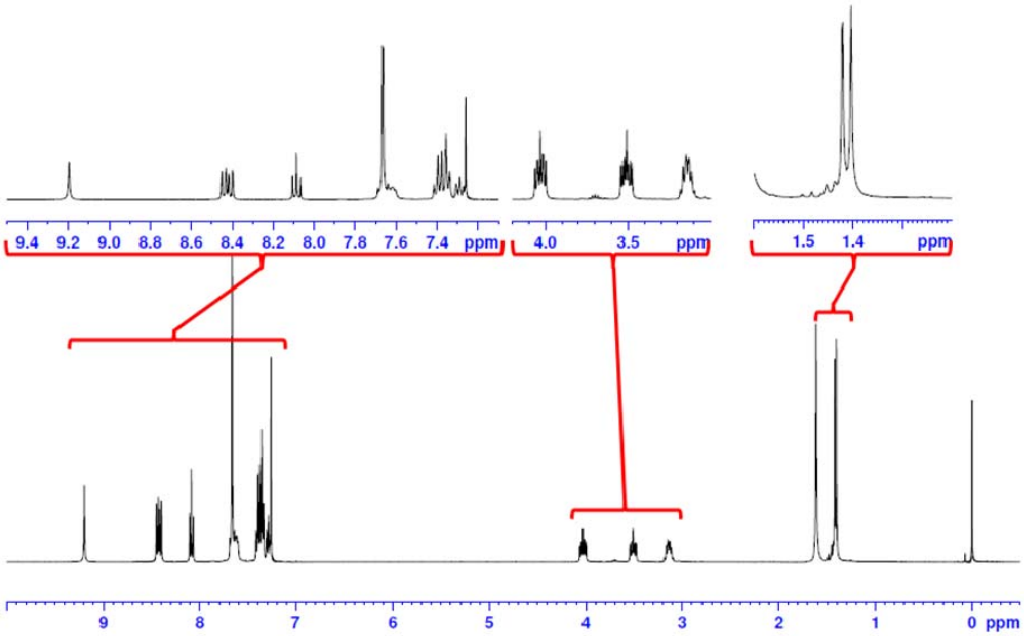

Figure S53. ^{1}H NMR spectrum of **L2^{RR}** in $CDCl_3$. The insets show the expansion of the corresponding region as indicated.

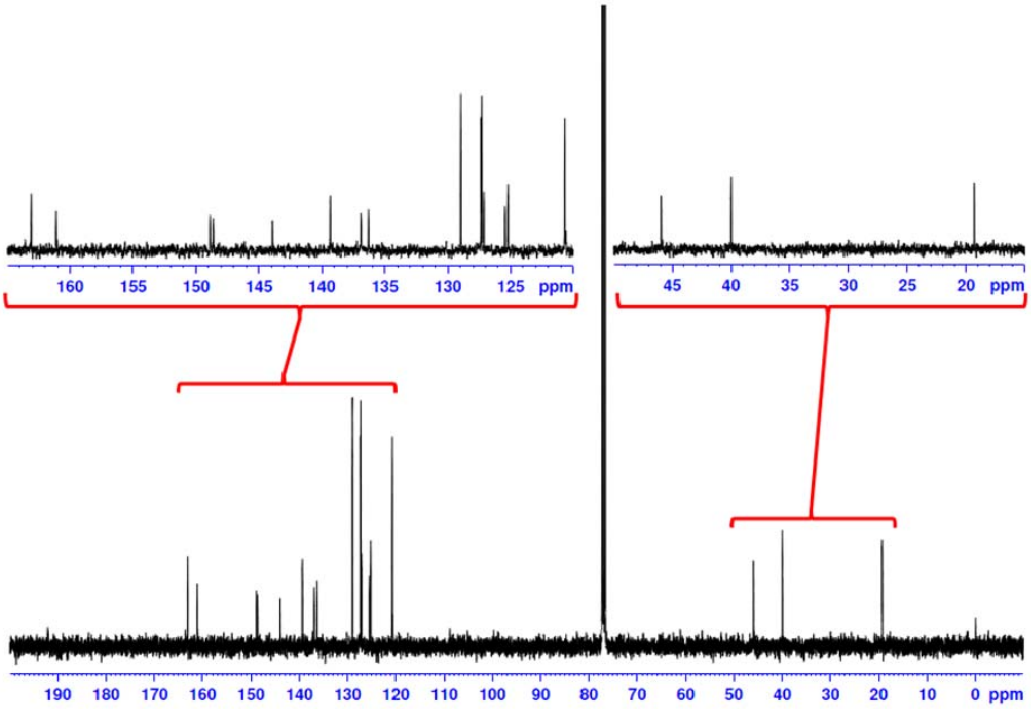

Figure S54. ^{13}C NMR spectrum of **L2^{RR}** in $CDCl_3$. The insets show the expansion of the corresponding region as indicated.

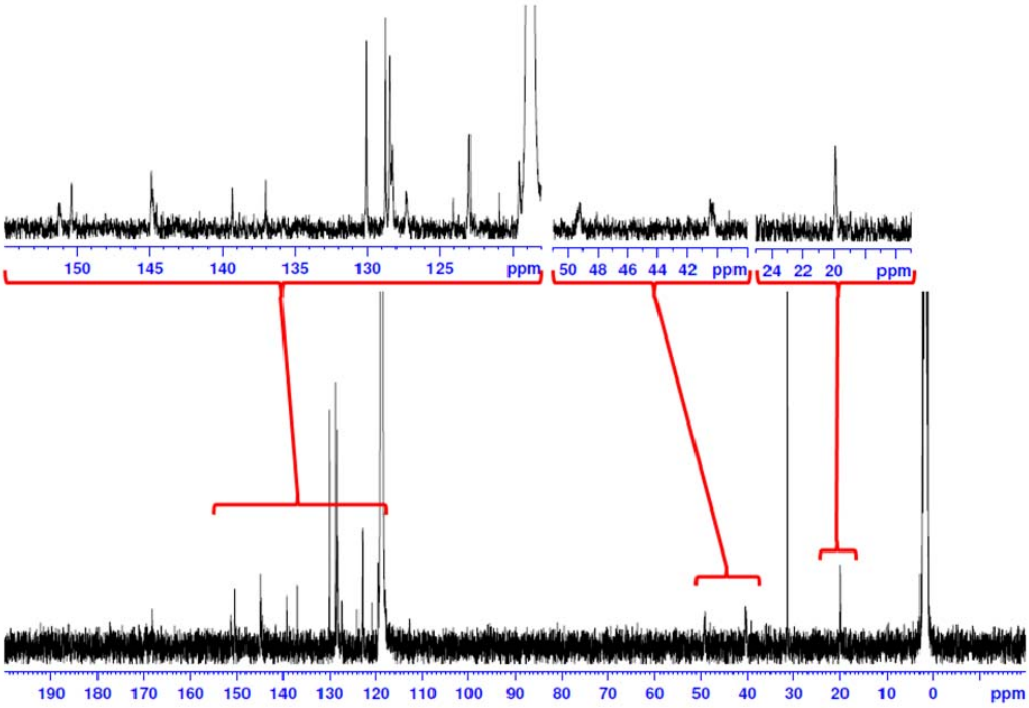

Figure S55. ^{13}C NMR spectrum of **[La$_2$(L2^{RR})$_3$](CF$_3$SO$_3$)$_6$** in CD_3CN. The insets show the expansion of the corresponding region as indicated.

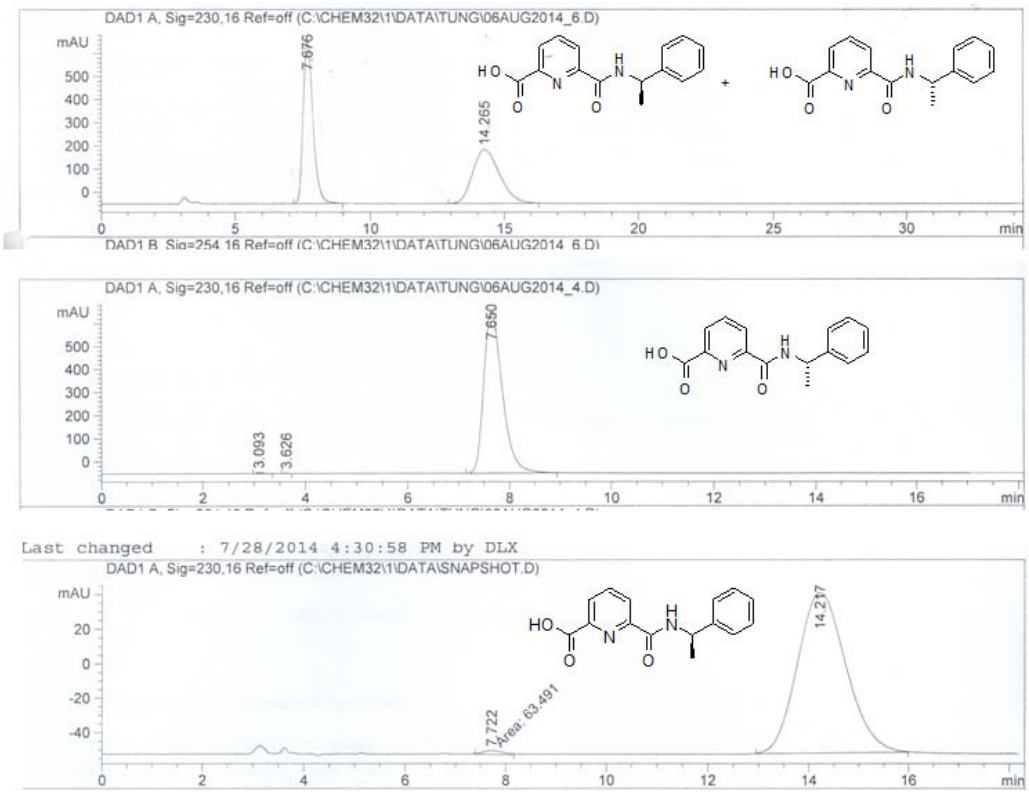

Figure S56. HPLC spectra of **1**^{S} and **1**^{R}**.**

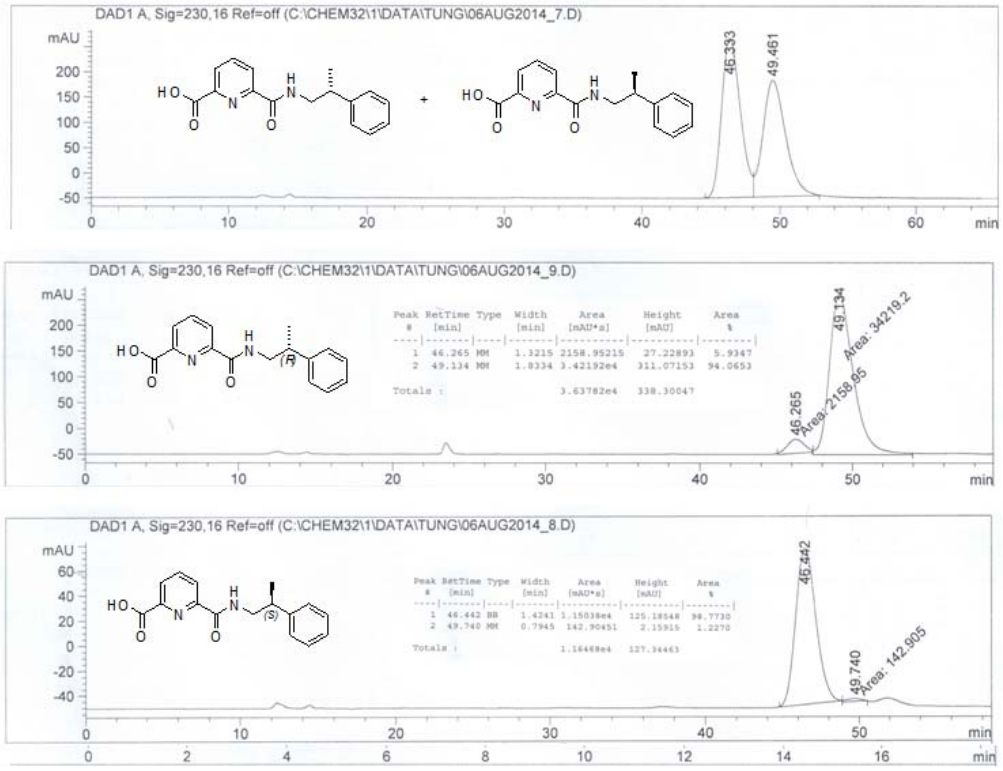

Figure S57. HPLC spectra of **2**^{S} and **2**^{R}**.**